RESEARCH

UDOT Keeping Utah Moving

Utah Department of Transportation - Research Division
4501 South 2700 West - P.O. Box 148410 - SLC,UT 84114-8410

Report No. UT-24.05

REPAIR OR STRENGTHENING OF BRIDGE DECKS WITH PARTIAL-DEPTH PRECAST DECK PANELS

Prepared For:

Utah Department of Transportation
Research & Innovation Division

Final Report
January 2024

DISCLAIMER

The authors alone are responsible for the preparation and accuracy of the information, data, analysis, discussions, recommendations, and conclusions presented herein. The contents do not necessarily reflect the views, opinions, endorsements, or policies of the Utah Department of Transportation or the U.S. Department of Transportation. The Utah Department of Transportation makes no representation or warranty of any kind, and assumes no liability therefore.

ACKNOWLEDGMENTS

The authors acknowledge the financial support provided by the Utah Department of Transportation. The authors would also like to thank the following companies for their contributions to the project: Forterra Structural Precast, Jack B. Parson Ready Mix Concrete, Sika AG, and Hilti Corporation.

TECHNICAL REPORT ABSTRACT

1. Report No. UT-24.05	2. Government Accession No.	3. Recipient's Catalog No.
4. Title and Subtitle REPAIR OR STRENGTHENING OF BRIDGE DECKS WITH PARTIAL-DEPTH PRECAST DECK PANELS		5. Report Date January 2024 6. Performing Organization Code N/A
7. Author(s) Chris P. Pantelides, Dylan T. Briggs		8. Performing Organization Report No. N/A
9. Performing Organization Name and Address Department of Civil and Environmental Engineering The University of Utah 110 Central Campus Drive Suite 2000 Salt Lake City, UT 84112		10. Work Unit No. 5H090 39H 11. Contract or Grant No. 21-8297
12. Sponsoring Agency Name and Address Utah Department of Transportation 4501 South 2700 West P.O. Box 148410 Salt Lake City, UT 84114-8410		13. Type of Report & Period Covered Final Report, Oct. 2020 – Jan. 2024 14. Sponsoring Agency Code PIC No. UT20.405
15. Supplementary Notes Prepared in cooperation with the Utah Department of Transportation and the U.S. Department of Transportation, Federal Highway Administration.		

16. Abstract

The primary objectives of this research project involve: (a) forensic analysis of composite deck samples from the I-15 800 South bridge; (b) replication of non-composite specimens for testing; (c) destructive testing of retrofitted non-composite deck samples; and (d) recommended solutions for the repair of bridges affected by debonding of the cast-in-place concrete section from the precast section without impacting traffic. Five retrofit methods were performed: (1) uni-directional carbon fiber reinforced polymer composite strips bonded to the bottom of the precast section; (2) proprietary mechanical shear anchors connecting the cast-in-place and precast section; (3) high modulus epoxy injection between the cast-in-place and precast sections; (4) nonproprietary shear anchors connecting the cast-in-place and precast sections; and (5) epoxy injection with proprietary shear anchors. Based on the research findings, the epoxy injection retrofit method is recommended to be the most effective solution for repairing bridge decks affected by debonding of the cast-in-place section due to interlayer delamination without impacting traffic.

17. Key Words Concrete, Delamination, precast, highway bridges, decks, overpass		18. Distribution Statement Not restricted. Available through: UDOT Research & Innovation Div. 4501 South 2700 West P.O. Box 148410 Salt Lake City, UT 84114-8410 www.udot.utah.gov/go/research		23. Registrant's Seal
19. Security Classification (of this report) Unclassified	20. Security Classification (of this page) Unclassified	21. No. of Pages 101	22. Price	

TABLE OF CONTENTS

LIST OF TABLES

LIST OF FIGURES

UNIT CONVERSION FACTORS

SI* (MODERN METRIC) CONVERSION FACTORS

APPROXIMATE CONVERSIONS TO SI UNITS

SYMBOL	WHEN YOU KNOW	MULTIPLY BY	TO FIND	SYMBOL
		LENGTH		
in	inches	25.4	millimeters	mm
ft	feet	0.305	meters	m
yd	yards	0.914	meters	m
mi	miles	1.61	kilometers	km
		AREA		
in^2	square inches	645.2	square millimeters	mm^2
ft^2	square feet	0.093	square meters	m^2
yd^2	square yard	0.836	square meters	m^2
ac	acres	0.405	hectares	ha
mi^2	square miles	2.59	square kilometers	km^2
		VOLUME		
fl oz	fluid ounces	29.57	milliliters	mL
gal	gallons	3.785	liters	L
ft^3	cubic feet	0.028	cubic meters	m^3
yd^3	cubic yards	0.765	cubic meters	m^3
		NOTE: volumes greater than 1000 L shall be shown in m^3		
		MASS		
oz	ounces	28.35	grams	g
lb	pounds	0.454	kilograms	kg
T	short tons (2000 lb)	0.907	megagrams (or "metric ton")	Mg (or "t")
		TEMPERATURE (exact degrees)		
°F	Fahrenheit	5 (F-32)/9 or (F-32)/1.8	Celsius	°C
		ILLUMINATION		
fc	foot-candles	10.76	lux	lx
fl	foot-Lamberts	3.426	$candela/m^2$	cd/m^2
		FORCE and PRESSURE or STRESS		
lbf	poundforce	4.45	newtons	N
lbf/in^2	poundforce per square inch	6.89	kilopascals	kPa

APPROXIMATE CONVERSIONS FROM SI UNITS

SYMBOL	WHEN YOU KNOW	MULTIPLY BY	TO FIND	SYMBOL
		LENGTH		
mm	millimeters	0.039	inches	in
m	meters	3.28	feet	ft
m	meters	1.09	yards	yd
km	kilometers	0.621	miles	mi
		AREA		
mm^2	square millimeters	0.0016	square inches	in^2
m^2	square meters	10.764	square feet	ft^2
m^2	square meters	1.195	square yards	yd^2
ha	hectares	2.47	acres	ac
km^2	square kilometers	0.386	square miles	mi^2
		VOLUME		
mL	milliliters	0.034	fluid ounces	fl oz
L	liters	0.264	gallons	gal
m^3	cubic meters	35.314	cubic feet	ft^3
m^3	cubic meters	1.307	cubic yards	yd^3
		MASS		
g	grams	0.035	ounces	oz
kg	kilograms	2.202	pounds	lb
Mg (or "t")	megagrams (or "metric ton")	1.103	short tons (2000 lb)	T
		TEMPERATURE (exact degrees)		
°C	Celsius	1.8C+32	Fahrenheit	°F
		ILLUMINATION		
lx	lux	0.0929	foot-candles	fc
cd/m^2	$candela/m^2$	0.2919	foot-Lamberts	fl
		FORCE and PRESSURE or STRESS		
N	newtons	0.225	poundforce	lbf
kPa	kilopascals	0.145	poundforce per square inch	lbf/in^2

*SI is the symbol for the International System of Units. Appropriate rounding should be made to comply with Section 4 of ASTM E380.
(Revised March 2003)

LIST OF ACRONYMS

CFRP	Carbon Fiber Reinforced Polymer
CIP	Cast-In-Place
HOV	High-Occupancy Vehicle
LVDT	Linear Variable Differential Transformer
PC	Precast Concrete
UDOT	Utah Department of Transportation

EXECUTIVE SUMMARY

The primary objectives of this research project included: (a) forensic analysis of composite deck samples from the I-15 800 South bridge; (b) replication of non-composite specimens for testing; (c) destructive testing of retrofitted non-composite deck samples; and (d) recommended solutions for the repair of bridges affected by debonding of the cast-in-place concrete section from the precast section without impacting traffic.

This report presents the results of the project during which seven full-scale experiments were carried out. The first series of five experiments used bridge deck specimens built in the laboratory where the precast section was located at the bottom of the deck and was reinforced with prestressing cables in the span direction.

The five retrofit methods were as follows: (1) uni-directional carbon fiber reinforced polymer composite strips bonded to the bottom of the precast section; (2) proprietary mechanical shear anchors connecting the cast-in-place and precast section; (3) high modulus epoxy injection between the cast-in-place and precast sections; (4) nonproprietary shear anchors connecting the cast-in-place and precast sections; and (5) epoxy injection with proprietary shear anchors.

The project's second phase evaluated the performance of two salvaged specimens obtained from the I-15 800 South bridge. The first salvaged specimen was tested without any retrofit solution, and the second salvaged specimen was retrofitted using the epoxy injection method.

Numerical models were developed for three cases to corroborate the laboratory testing: a delaminated deck panel with no retrofit, a nonproprietary shear anchor retrofit, and an epoxy injection retrofit. Similar to laboratory testing, the numerical model concluded that the epoxy injection increases the deck panels' stiffness significantly, creating a more composite behavior.

After all of the testing and analysis, the research team recommends that the epoxy injection retrofit method is the most effective for similarly constructed bridge deck panels affected by this type of debonding behavior.

1 INTRODUCTION

1.1 Problem Statement

The I-15 over 800 South bridge in Salt Lake City, Utah, experienced an unexpected blow-through, requiring an emergency closure and repair, on March 24, 2019, as shown in **Fig. 1.1**. After inspection, it was determined that other sections of the deck were in danger of a similar failure. The likely cause of failure was delamination and deterioration of the interface between the cast-in-place section and precast section. The Utah Department of Transportation (UDOT) developed a repair plan, which consisted of removing complete sections of the deck and replacing the damaged concrete with a rapid-hardening hydraulic cement concrete mix. Three lanes were closed over the 800 South bridge, and the bridge was re-opened on March 25, 2019. Although this is a viable repair method, it significantly impacts traffic and is a high-cost repair method.

Figure 1.1 Blow-through of deck panel at I-15 and 800 South bridge (credit: UDOT)

1.2 Objectives

The primary objectives of the project involved: (a) forensic analysis of composite deck samples from the I-15 800 South bridge; (b) replication of non-composite specimens for testing; (c) destructive testing of retrofitted non-composite deck specimens; and (d) recommended solutions for the repair of bridges affected by debonding of the cast-in-place concrete section from the precast section without impacting traffic.

1.3 Literature Review

Prior to any testing, a preliminary literature review was performed by the research team to determine the extent of similar problems affecting partial-depth bridge construction. Several state transportation agencies have identified that the composite action of partial-depth construction is an area of significant concern.

In 2005, a study conducted by Washington State Transportation Center determined that the most common problems with the use of partial-depth panel decks is cracking of the cast-in-place portion of the deck at both the transverse joints between panels and at locations where the panels are supported by girders. As a result of this research, WSDOT only uses partial-depth slabs in dead load positive moment regions of the bridge deck (Hieber et al., 2005).

One of the few studies that addressed the composite action of the cast-in-place (CIP) and precast concrete (PC) portions of bridge decks was conducted in 2006. The I-393 bridge over the Merrimack River in New Hampshire was the emphasis of this study, and the research concluded that the bond between the two separate sections did, in fact, behave compositely. They also discovered that the bond was improving over time, and the panels were adequately transferring the traffic load without causing reflective cracking (Whittemore et al., 2006).

It was observed by the Missouri Department of Transportation that oxidation of embedded rebar components within the CIP section were responsible for spalling-induced cracks of bridge decks. Several methods for new construction were evaluated including the addition of fibers or corrosion inhibitors, or an increase of the steel reinforcement of the CIP section. The methods were then evaluated using fundamental laboratory studies and numerical analysis. The study concluded that cracks usually only extend to partway through the CIP portion of the deck slab and that cracking is mainly attributed to shrinkage at the joints between precast panels. While these failures are not immediately concerning, the cracks allow for the ingress of moisture and other surface contaminants ultimately influencing the bond between the two separate sections. Sneed et al. (2010) recommended the following three methods for non-structural repair to prevent the penetration of water and chlorides into the panel: (a) sealing the surface cracks; (b) near surface reinforcement or pinning; and (c) epoxy injection between the CIP and PC interface. The method

of epoxy injection was recommended for use at panel joint locations since those are the areas that are anticipated to suffer from this type of delamination failure.

A long span bridge on State Highway 75 (SH 75) using partial-depth construction was evaluated by researchers in 2018 after the Texas Department of Transportation discovered that it was vibrating excessively. The bridge was constructed using bridge deck specifications similar to those used by UDOT. Researchers were able to identify extensive transverse and longitudinal cracks on top of the bridge deck and several potholes had already been filled. Furthermore, the team identified using ground-penetrating radar that roughly 30% of the bridge was delaminated and that most of the delamination occurred toward the girder locations (Efaz et al., 2022).

None of the studies evaluated for this review tested any method for retrofitting partial-depth bridge decks. Sneed et al. (2010) suggested the use of epoxy injection at the deck joints, but no analysis of its effectiveness was tested. This study aims to fill the gap in research by testing minimally invasive retrofit techniques for partial-depth bridge construction and verifying their effectiveness using numerical modeling.

1.4 Outline of Report

This report is compiled to explain the tasks that were accomplished by the research team to evaluate the effectiveness of seven retrofit methods.

Chapter 2 explains how the non-composite behavior was replicated and how the test samples were constructed.

Chapter 3 presents the various retrofit options and how those methods were applied to each of the test specimens.

Chapter 4 describes how the specimens were tested. The instrumentation and test equipment are explained along with the test procedure.

Chapter 5 presents an in-depth analysis of the test data.

Chapter 6 presents the testing and retrofit of the salvaged panels from the 800 South bridge deck.

Chapter 7 includes a numerical evaluation of the laboratory tests using finite element methodology.

Chapter 8 summarizes the research findings and presents a recommendation for future repairs involving similarly constructed concrete deck systems.

2 DESIGN AND CONSTRUCTION OF TEST SPECIMENS

It was important for the research team to successfully replicate the behavior of the 800 South bridge in a controlled laboratory setting. The design of the test specimens involved taking measurements from the salvaged panels provided by UDOT and technical drawings from other similar bridge construction projects. The precast panels were supplied by Forterra Structural Precast; a schematic drawing of those panels can be found in **Fig. 2.1**. The cast-in-place section of the composite deck system was constructed by the research team at the University of Utah Structural Engineering Laboratory.

The test specimens were constructed according to the drawings developed during the forensic study of the 800 South bridge salvaged panels. To prevent the cast-in-place (CIP) concrete from properly adhering to the precast (PC) panel, vegetable oil was applied, as seen in **Fig. 2.2**. The application of vegetable oil serves to create an upper bound for testing (worst-case scenario). The precast panels provided by Forterra were 8-feet by 8-feet in dimension. Before the panels were tested, they were cut into 4-foot by 8-foot specimens. Additional information regarding the precast panel is provided in **Table 2.1** The cast-in-place portion contained concrete with a 28-day compressive strength of 3,700 psi. Additional compressive strength tests were performed on panel test days with an average compressive strength of 6,500 psi.

Table 2.1 Precast panel specifications

Precast Panel Specifications		
f'c	6,000	psi
f'ci	4,500	psi
fpu	270,000	psi
Fi	17.2	Kip
Ff	14.3	Kip

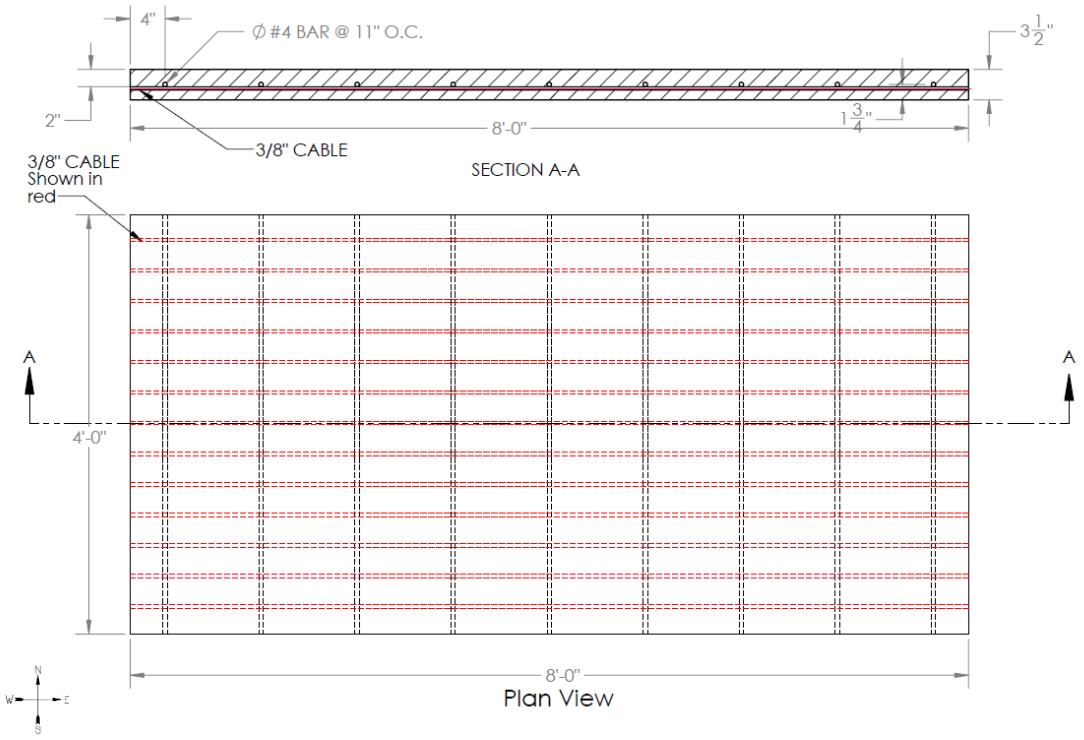

Figure 2.1 Precast panel schematic drawing for conventional panels.

Figure 2.2 CIP section ready for casting with vegetable oil applied to the precast surface.

3 RETROFIT OF TEST SPECIMENS

Chapter 3 describes the different methods of retrofit and their application to the specimens. Schematic diagrams, along with the rationale behind the method selection are also included.

3.1 Epoxy Injection Retrofit

Epoxy injection has been successfully used as a structural repair option for many years. The theory behind this method of retrofit is to effectively fill the space between the cast-in-place section and precast section of the panels with a high modulus two-part epoxy and permanently bond the two surfaces, preventing separation and forcing the two sections to behave compositely. This method of retrofit also prevents the intrusion of water and other contaminants.

To prepare the panel for epoxy injection, it was necessary to determine the extent to which the epoxy could spread between the cast-in-place and precast sections. A simple test was performed using a flat granite slab and 8.5 fluid ounces of water, the volume of one epoxy tube. Water was chosen for the test because the epoxy used has a similar viscosity to that of water. The water was slowly poured over the granite surface and the distribution of the liquid was recorded, as shown in **Fig. 3.1**. The distribution of liquid determines how many injection ports would need to be prepared. With the information obtained from the liquid test, it was determined that eight injection sites spaced according to **Fig. 3.2** would allow the epoxy to permeate between the cast-in-place and precast sections of the panel.

Figure 3.1 Liquid dispersion test.

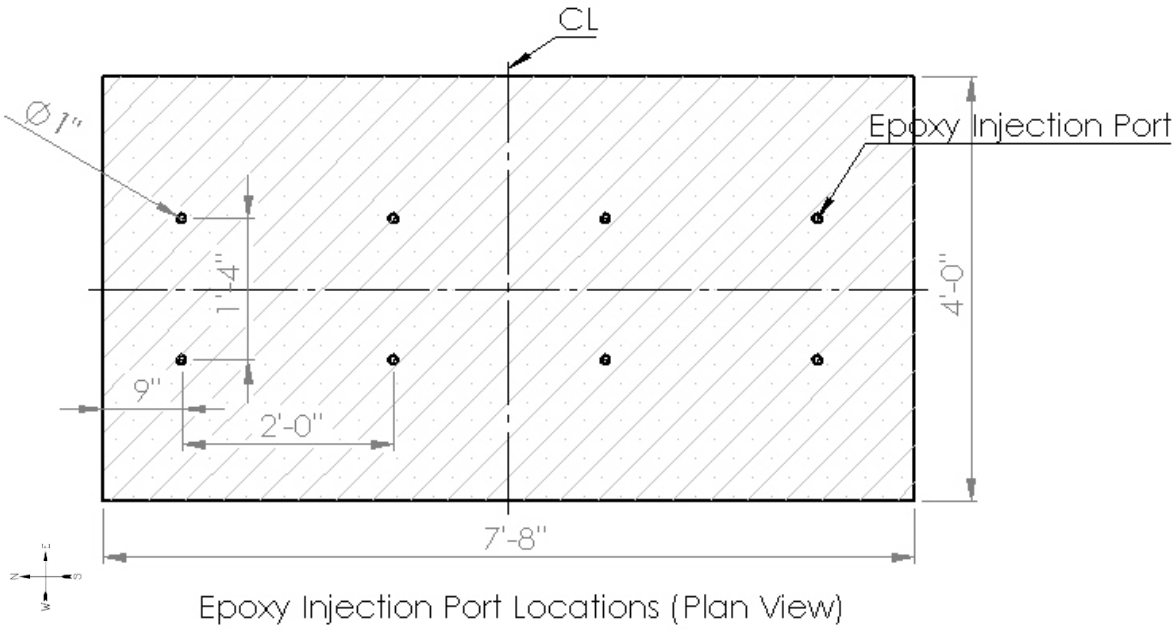

Figure 3.2 Schematic diagram of epoxy port sites (plan view).

Eight 1-in. diameter holes were drilled into the top of the deck panel and cleared of debris, and the one-way injection ports were installed according to the manufacturer's specifications. A schematic drawing in **Fig. 3.2** illustrates the port spacing relative to the test panel. The installation of the ports is shown in **Figs. 3.3 to 3.5**. It is important to note that the retrofit was performed from the top surface of the cast-in-place portion of the deck, the street surface. This was done for the purpose of testing only and should not be attempted in the field. Performing the retrofit from the surface allows for the epoxy to fill the void more efficiently between the panels. The epoxy was injected until it was observed exiting from the void between panel sections. It is important to note that no effort was made to remove the vegetable oil from between the deck panels.

Figure 3.3 Epoxy injection port hole preparation.

Figure 3.4 Application of adhesive to epoxy injection port.

Figure 3.5 Epoxy injection port installed.

3.2 Proprietary Mechanical Shear Anchor Retrofit

The second method of retrofit involved the use of mechanical anchors. The principle behind the use of these anchors, as it applies to the deck panels, is to mechanically attach the cast-in-place and precast sections of the panel together and force them to behave compositely. The anchors also prevent any lateral movement of the weaker cast-in-place section. The proprietary anchor does not require clearing concrete dust from the installation site, and the anchors have been designated by the manufacturer as suitable for overhead installation.

The number of anchors used for the retrofit was determined as follows. Based on the size of the panel (4 ft–0 in. x 7 ft–8 in.) and the clear span, the horizontal shear capacity was determined based on the flexural capacity of the composite panel. Thus, it was determined that two rows of three anchors for a total of six anchors was a reasonable amount for actual bridge decks, as shown in **Fig. 3.6**. A total of six 3/4 in. anchors were used. Each anchor was inserted to a depth of 6 in. In an actual bridge deck, this would correspond to an average spacing of 24 in. in each direction. This corresponds to an increase in shear capacity of approximately 12 kip or an increased applied load of 24 kip. It was also assumed that this increase in shear capacity would prevent the precast and cast-in-place sections of the panel from separating apart, and it was expected that the panel would behave in a composite manner.

The installation of the anchors can be seen in **Fig. 3.7**. For the purpose of this study, the installation of the anchors was performed with the entire test panel inverted. In the field, the installation of shear anchors would be performed from the underside of the compromised bridge deck of the overpass; overhead installation of epoxy, when performed correctly, would provide similar performance. Prior to testing the panel, it was turned over into the correct orientation. The process involves drilling into the panel, followed by an adhesive intended to secure the anchor in place. The anchor is fitted with a series of ridges along the embedded surface, as shown in **Fig. 3.8**; these ridges serve to increase the amount of available surface area that will bond with the epoxy. Once the adhesive had cured, the bolts were tightened to the manufacturer's specifications, as shown in **Fig. 3.9**, and the panel was ready to be tested. The panel with the most severe delamination was chosen as a candidate for the shear anchors to determine the effectiveness of this solution. When the anchors on the test panel were tightened, the gap between

the CIP section and precast section was reduced from 0.50 in. to approximately 0.25 in. This panel was the most compromised panel prior to testing, and it is believed that its ability to resist the applied load was reduced in part to premature cracking.

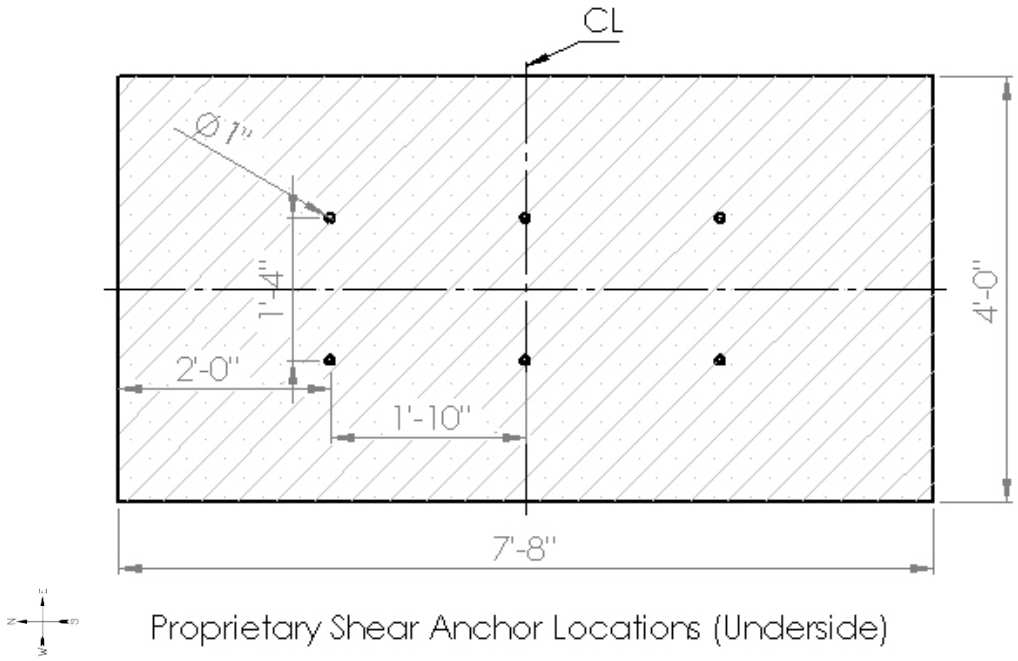

Figure 3.6 Schematic drawing of shear anchor placement. (plan view)

(a) (b)

Figure 3.7 Proprietary shear anchor installation: (a) drilling 1-in. hole; and (b) injection of epoxy.

Figure 3.8 Proprietary anchor being placed into the concrete panel.

Figure 3.9 Researcher tightening the proprietary anchor to manufacturer's specifications.

3.3 Carbon Fiber Reinforced Polymer Strip Retrofit

This retrofit included the use of a proprietary solution. It is comprised of a unidirectional carbon fiber composite cured laminate and is bonded to the concrete surface using a high modulus two-part epoxy. The retrofit has been used successfully in strengthening parking structures including slabs and beams. The composite laminate has a high tensile strength that can resist large structural deformations.

The number of CFRP composite strips used for the retrofit was determined as follows. Based on the retrofit using the proprietary anchors, the corresponding increase in the applied load was 24 kip. This resulted in an increase in flexural capacity of the composite panel of 2,260 kip-in. Assuming a strain effectiveness of the CFRP strips of 66% compared to the CFRP composite ultimate strain and including the contribution of the prestressing cables, it was found that two CFRP composite strips would provide the same increase in bending moment capacity and horizontal shear as the proprietary anchors. The schematic drawing in **Fig. 3.10** shows the spacing of the CFRP strips. In addition to the increase in bending moment and horizontal shear capacity, it was anticipated that the deflection of the panel would decrease, keeping the precast and cast-in-place panels from separating apart.

The installation of the carbon fiber strip was overseen by a trained product representative. The product involves careful surface preparation; the panel was roughened, as shown in **Fig. 3.11(a)** and degreased, as shown in **Fig. 3.11(b)**. The two-part epoxy was then mixed according to the manufacturer's specification while the bonding surface was degreased and then applied to both the concrete and the CFRP strip. The amount of epoxy deposited onto the strip was controlled using the fixture shown in **Fig. 3.12**. The installation of the CFRP strip was performed in the laboratory with the entire test panel inverted. Performing the installation in this fashion ensured that the product was installed as correctly as possible. In the field, this type of installation is not possible, but the high viscosity epoxy recommended by the manufacturer is able to hold the strip in place on the underside of the bridge deck until it is properly cured. **Fig. 3.13** shows the CFRP strip after installation and prior to testing.

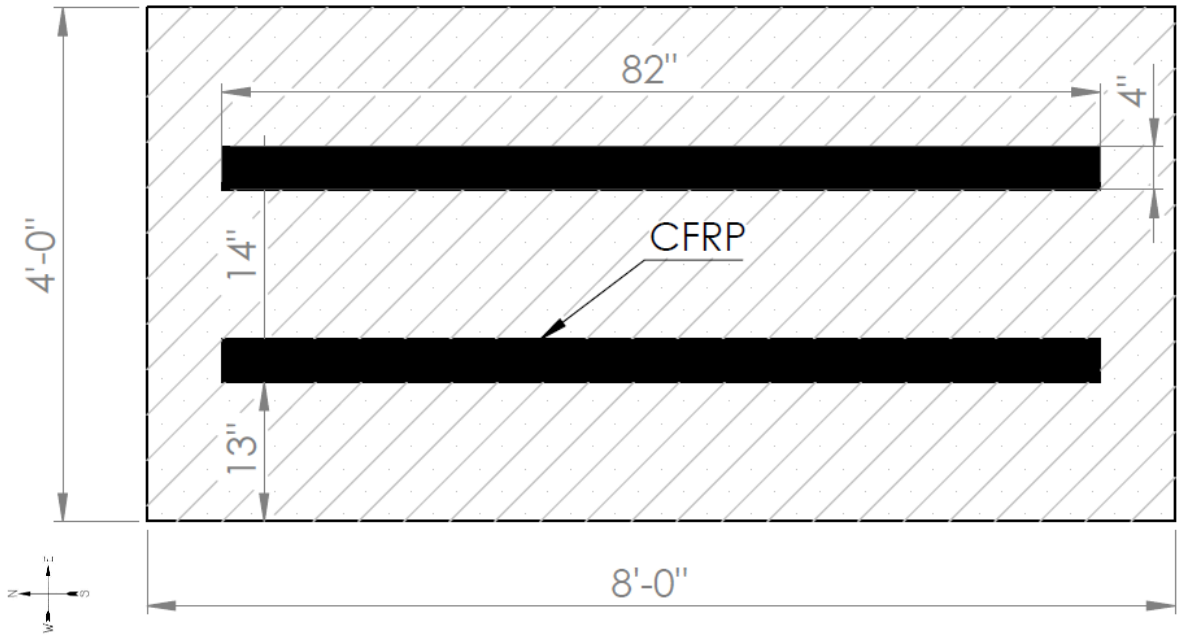

Figure 3.10 Schematic drawing of CFRP location on precast panel.

(a) (b)

Figure 3.11 Test panel preparation: (a) surface roughening; and (b) surface panel degreasing.

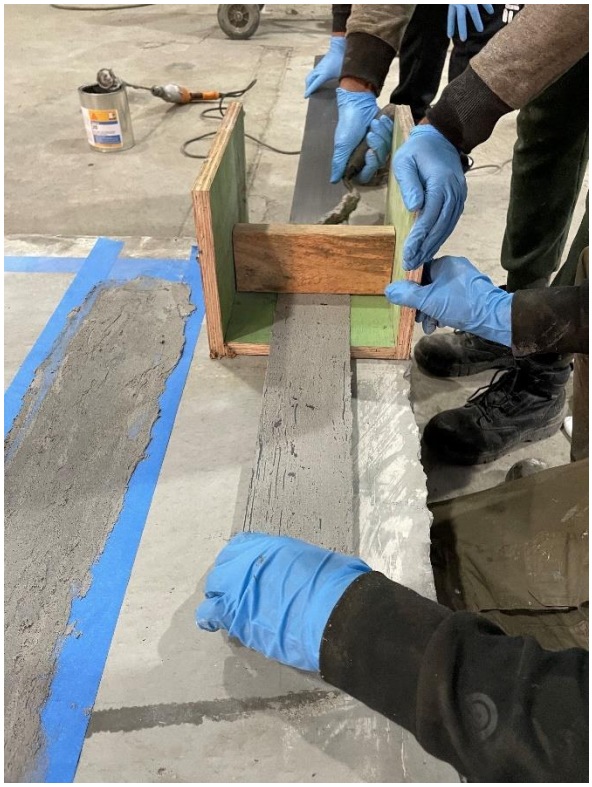

Figure 3.12 CFRP strip being pulled through epoxy depth control fixture.

Figure 3.13 Underside of test panel with CFRP strip installed.

3.4 Nonproprietary Shear Anchors

Several 105 ksi threaded rods with a zinc corrosion resistant coating were also used as mechanical shear anchors similar to the proprietary product from *Section 3.2*. The anchors were installed according to the schematic drawing shown in **Fig. 3.14**. A nonproprietary anchor is shown in **Fig. 3.15** before installation. To improve the performance of these anchors they were offset 12 in. from the centerline. The smaller diameter of the threaded rod required the installation of eight total anchors to achieve the required horizontal shear capacity of the composite panel. The anchors measured 6 in. in length and were embedded until they were flush with the precast panel. The installation procedure is identical to that for the proprietary shear anchors from *Section 3.2*.

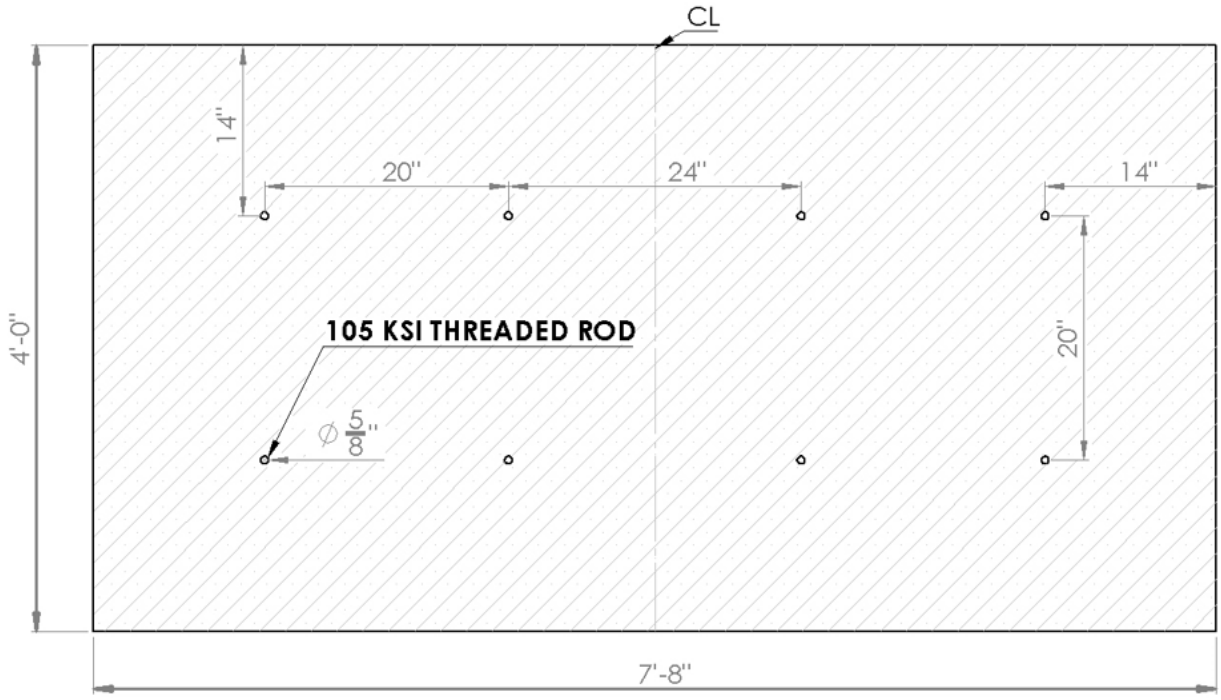

Figure 3.14 Nonproprietary shear anchor schematic drawing (underside of test panel).

Figure 3.15 Nonproprietary shear anchor prior to installation.

3.5 Epoxy Injection with Proprietary Mechanical Anchors

With the information obtained from the previous tests, a hybrid method was used that employed epoxy injection along with proprietary mechanical shear anchors. This retrofit method aimed to reduce the amount of epoxy required to fill the gap by first closing the gap using the mechanical anchors, and improve composite action. The anchors and epoxy were installed according to the schematic drawing shown in **Fig. 3.16**. Tightening of the anchors resulted in no observable closure of the gap between the cast-in-place and precast sections of the panel. The underside of the panel with the installed retrofits is given in **Fig. 3.17**.

This method of retrofit is difficult to perform due to the curing limitations of the epoxy. The following describes the steps that must be completed prior to loading:

1. Drill all of the holes for the epoxy injection ports and the shear anchors.
2. Install the epoxy injection ports and the shear anchors using the corresponding epoxy. Allow 24 hours to cure.
3. Install and tighten all bolts on the shear anchors.

4. Inject the high modulus epoxy through the injection ports, as shown in **Fig. 3.18** and wait an additional 24 hours.

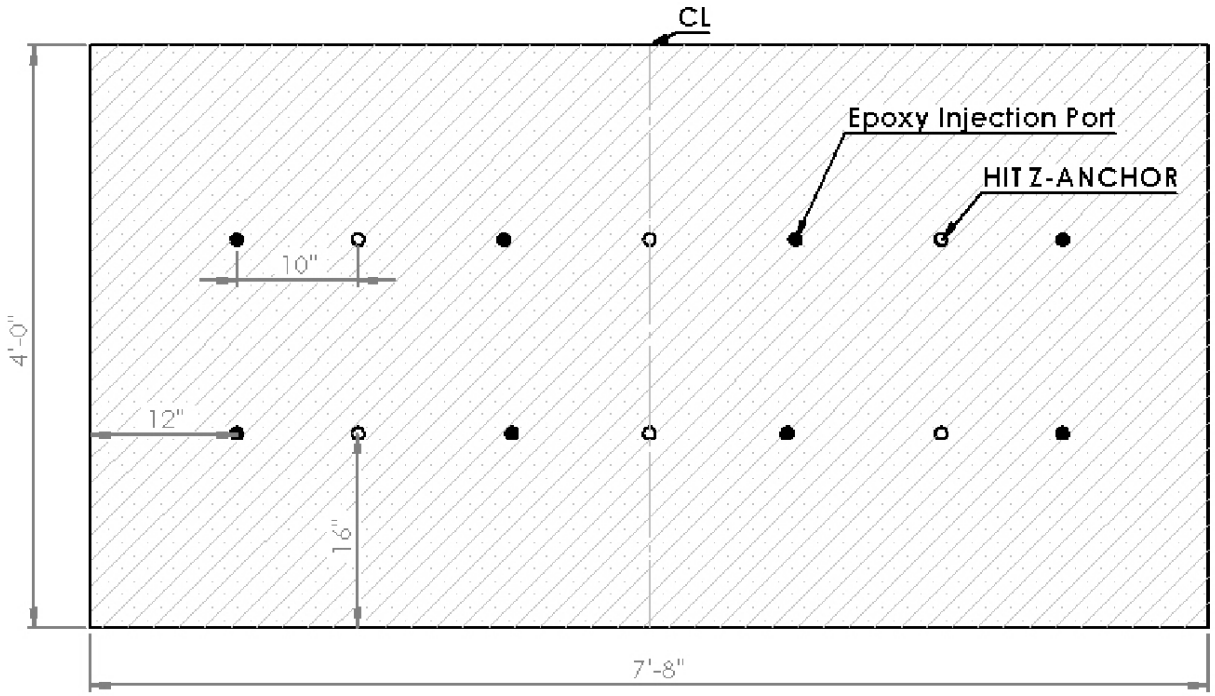

Figure 3.16 Epoxy injection with proprietary mechanical anchors schematic drawing (underside of panel).

Figure 3.17 Completed installation of proprietary anchors and epoxy injection ports.

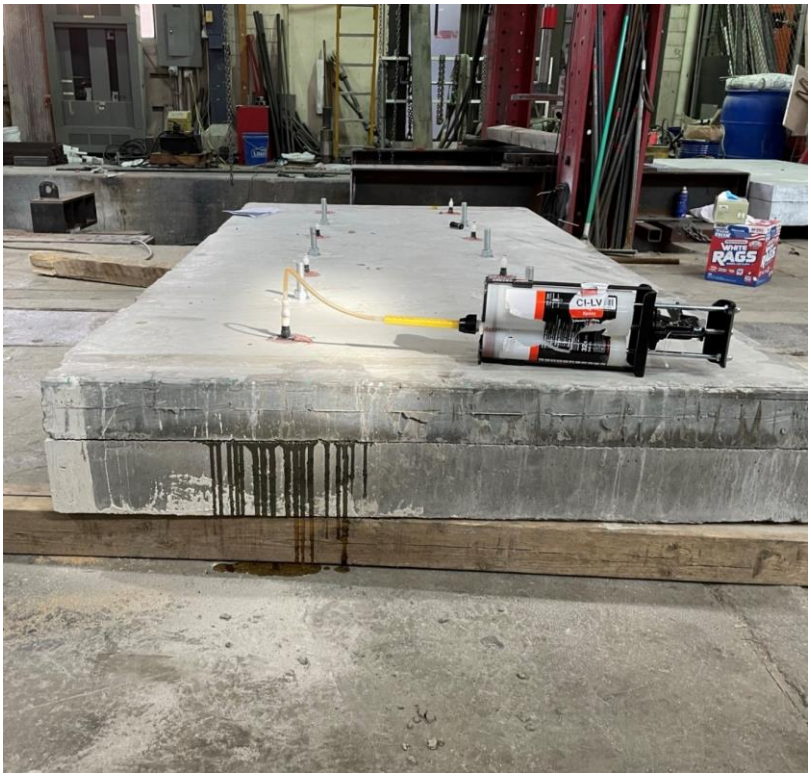

Figure 3.18 Epoxy injection leaking from panel.

3.6 Comparison of Installation of Retrofit Methods

Each retrofit method presented its unique challenges for installation. The most efficient installation involved the two types of shear anchors; not only was the installation fast but it also required minimal equipment to perform. The installation that required the most attention to detail was the CFRP strips. The epoxy mortar had to be installed at a very specific depth which was difficult to maintain. The surface preparation for the CFRP strips was time consuming. The most challenging method of retrofit for this style of construction was the epoxy injection. The effectiveness of the epoxy injection is not immediately apparent during the installation phase. In the field, it would be impossible to determine what areas of the panel had experienced interlayer delamination. The panel treated with the epoxy injection retrofit contained areas that were not delaminated but could not be seen until a dissection was performed after testing. Working from the underside of a bridge would also eliminate the benefit of gravity to effectively disperse the adhesive. Finally, it is not possible to accurately confirm if the entire void has been filled with the epoxy resulting in uneven distribution.

4 TESTING PROCEDURE

Chapter 4 outlines in detail the testing procedure used to evaluate each of the retrofitted panels. The instrumentation, test setup, and loading procedure are all described herein.

4.1 Test Setup

All testing was performed at the University of Utah's Structural Laboratory. The testing was carried out using a test frame with an ability to resist 500-kip in each direction. A 120-kip servo-controlled hydraulic actuator was positioned vertically to apply a displacement-controlled loading protocol at the center of each panel.

The panels were positioned on the top of two steel rollers to allow for smooth movement and rotation of each panel as it responded to the imposed displacement. **Fig. 4.1** shows a schematic drawing of the panel and its position on the test fixture. For each test, the clear span was kept at a consistent 87-in. length. The load was applied at the center of each panel through a 1-inch-thick steel plate with the dimensions shown in **Fig. 4.2**.

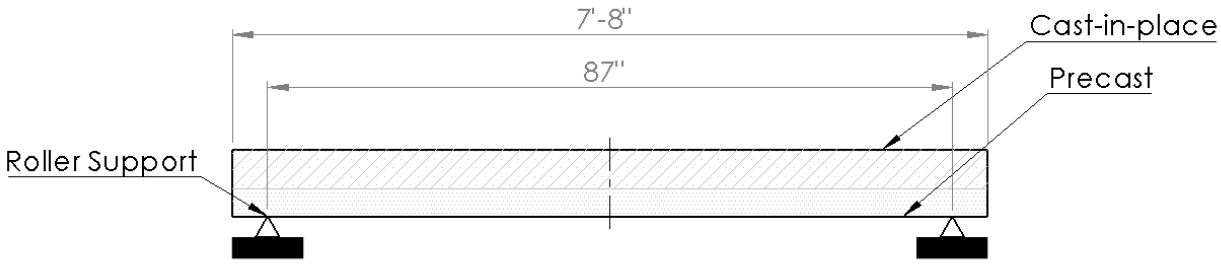

Figure 4.1 Test frame schematic drawing (profile view).

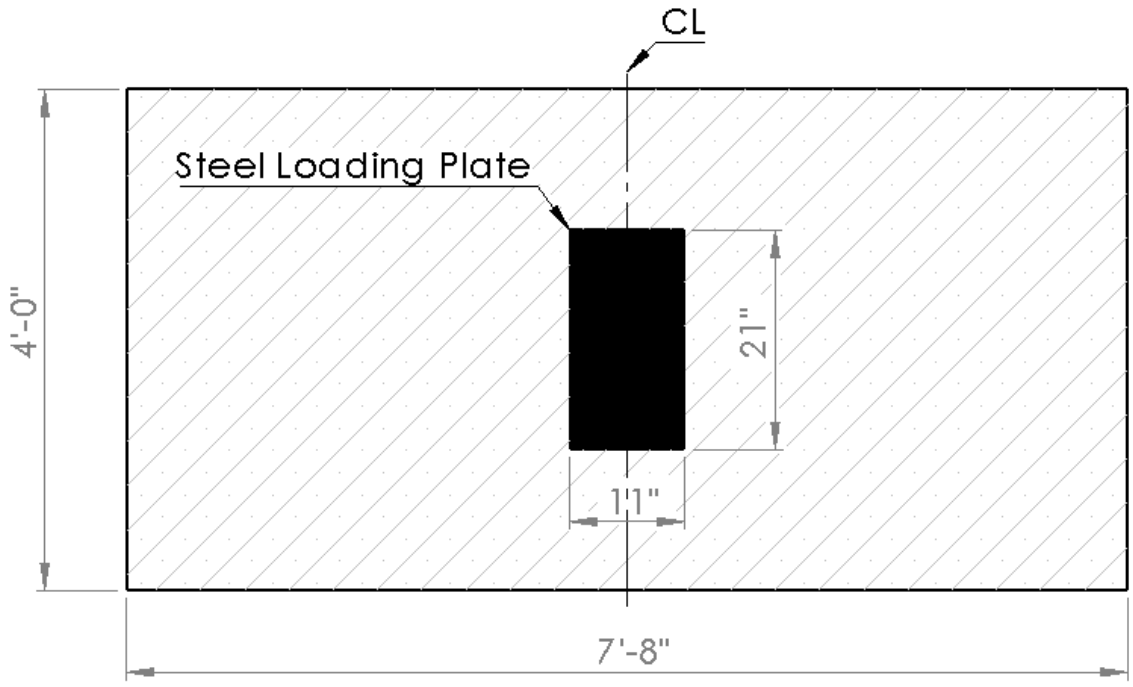

Figure 4.2 Schematic drawing of concrete panel with loading plate shown (plan view).

4.2 Instrumentation

Three linear variable differential transformers (LVDT) were used to capture the linear movement of the test specimens at strategic locations on the panel as it responded to the applied loading. Two LVDTs (north and south LVDT) were placed at the north and south extremes of the specimen to measure the separation of the cast-in-place section from the pre-cast section, as shown in **Fig. 4.3**. Another LVDT (midspan LVDT) was placed on the underside of the panel at midspan to capture the total deformation. The applied force was recorded using a calibrated load cell between the hydraulic actuator and test panel.

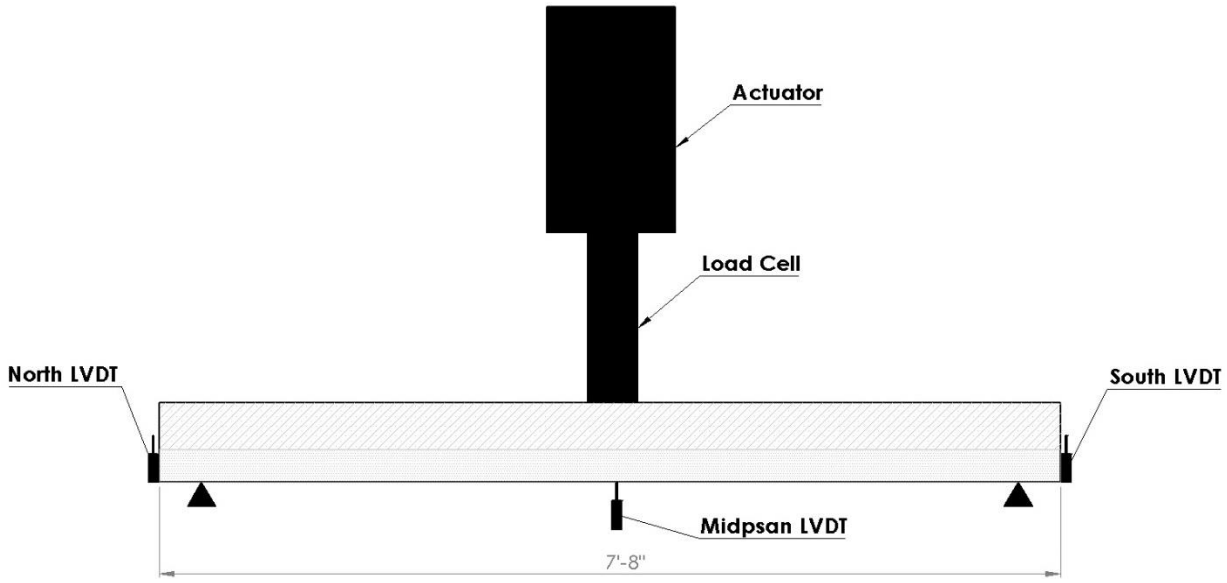

Figure 4.3 Schematic drawing of the instrument locations.

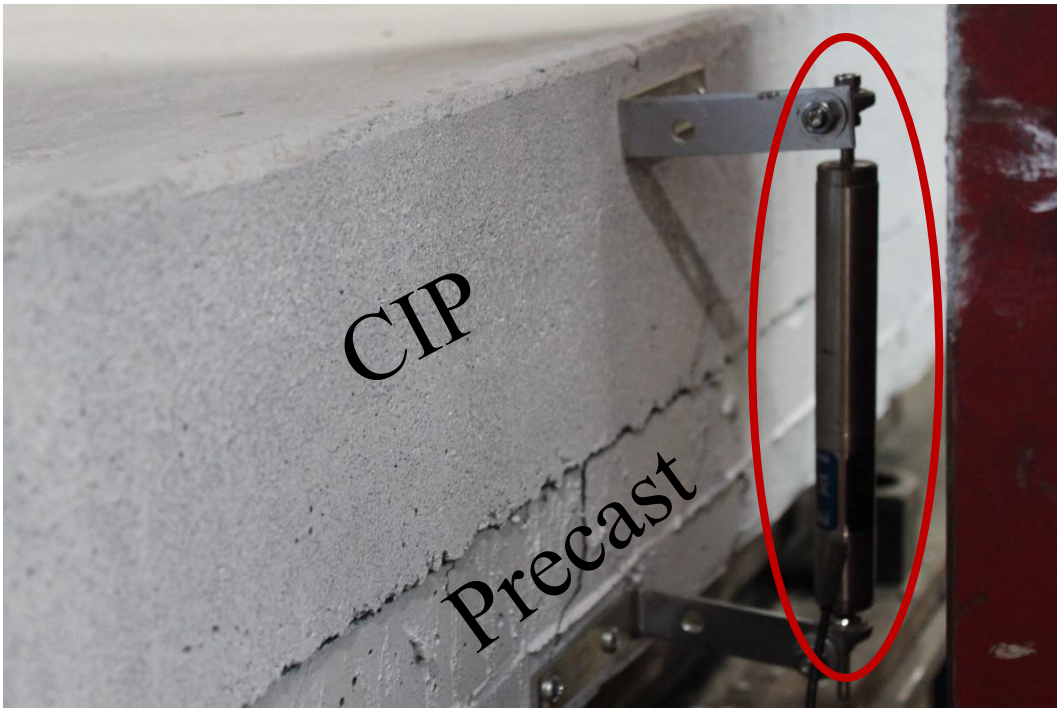

Figure 4.4 LVDT location on south side of test panel.

4.3 Displacement History

A monotonic half-cyclic displacement-controlled force was applied to each of the test specimens. **Fig. 4.5** shows the displacement applied at each interval using the initial load protocol. The displacement increased at a rate of 0.2-in./sec with a 30-sec dwell between each loading cycle; at 1.2-in. displacement, the loading rate was increased to 0.4-in./sec with the same 30-sec dwell between cycles.

The load protocol was modified to include additional load cycles at smaller displacements as shown in **Fig. 4.6**. This protocol was applied to the nonproprietary shear anchor panel, the proprietary shear anchor with epoxy injection panel, the salvaged with no retrofit panel, and the salvaged panel with the epoxy retrofit. The smaller displacements were included for these specimens to capture the test panel behavior under real-world conditions.

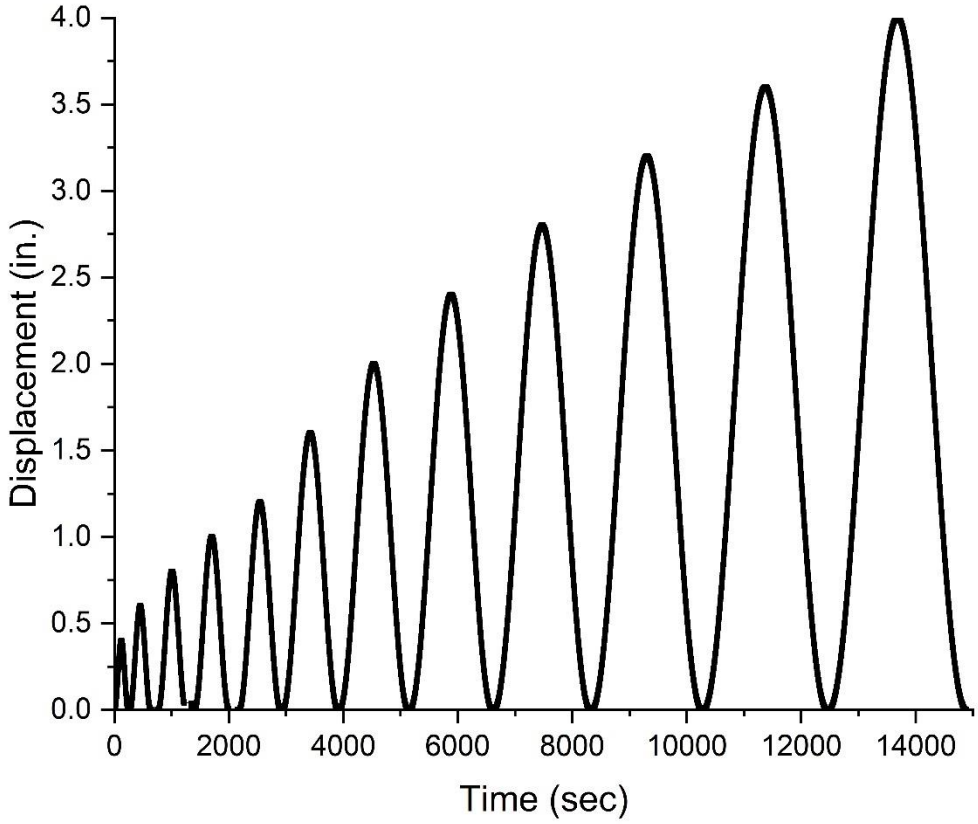

Figure 4.5 Initial loading protocol.

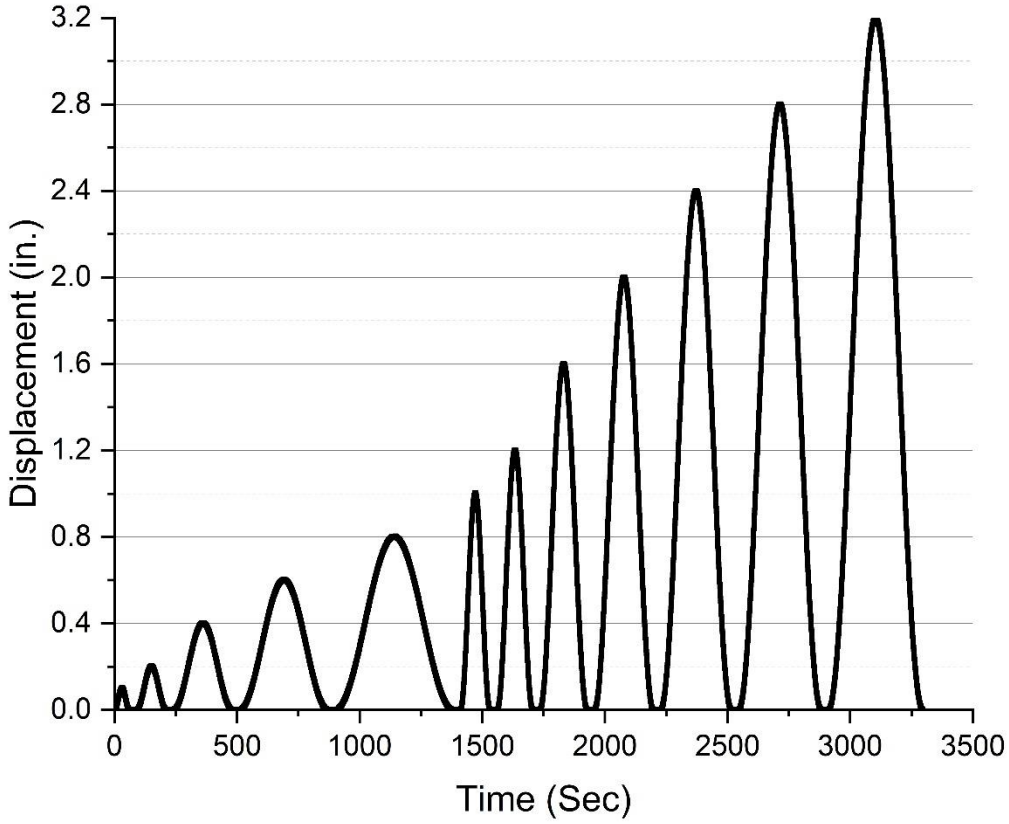

Figure 4.6 Secondary loading protocol.

5 TEST RESULTS AND ANALYSIS

The response of each specimen is described within this chapter. Each section compares the retrofitted specimen's response to the test panel that was created with an initial interlayer delamination with no retrofit.

5.1 Test Panel with No Retrofit (Control)

To generate a baseline for comparison, a delaminated panel without any retrofit was tested as the control according to the parameters outlined in *Chapter 3.* **Fig. 5.1** shows the initial delamination of the control panel at the northwest and southwest corners respectively, prior to initiating the loading sequence. This initial delamination was created by applying vegetable oil before casting the cast-in-place concrete, as explained in *Chapter 2*. It is important to note that all measurements made using the LVDTs do not include this initial delamination.

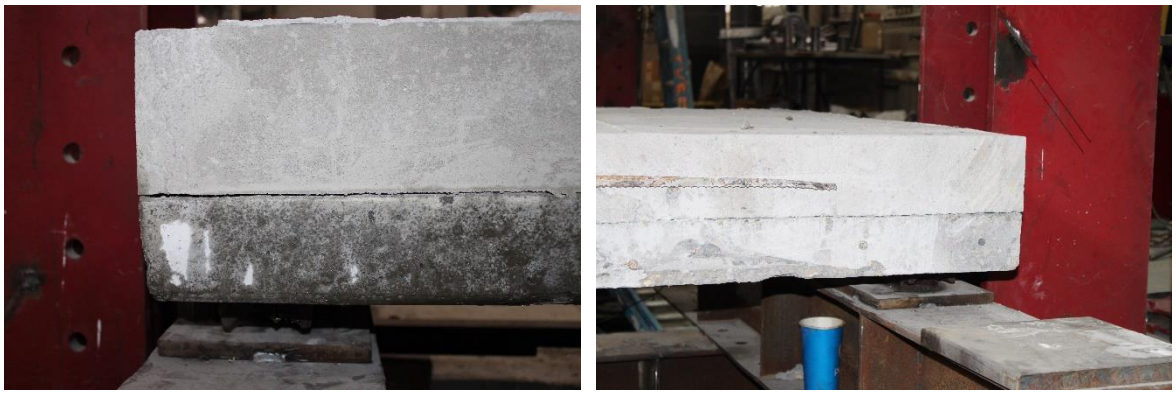

Figure 5.1 Unmodified deck panel prior to starting testing with delamination shown. Southwest; left, Northwest; right.

The unmodified deck panel behaved in a manner consistent with a non-composite specimen. The precast and CIP sections of the panel visually appeared to be acting independently of one another. At the end of the sixth displacement cycle (1.2 in.), the delamination became immediately visible. **Fig. 5.2** captured the separation of the two panels at the southwest corner after the 1.2-in. displacement cycle. The delamination continued to grow as anticipated; **Fig. 5.3** shows the panel at 2.4 in. of displacement with the anticipated debonding behavior.

The most critical information captured from each test cycle is shown in **Fig. 5.4**. This graph displays the specimen displacement at the north and south extremes as recorded by the

LVDTs. It is evident in this graph that as the applied displacement increases, the panel is unable to fully recover, and the gap continues to grow. Not only does the delamination increase the deflection, but the deflection becomes permanent, and the specimen's strength is ultimately compromised. The hysteresis curves of the entire loading protocol have been included along with the point of delamination in **Fig. 5.5**. This figure shows in a red circle the point where delamination became visible (1.2 in.).

The LVDT plot in **Fig. 5.4** indicates that internal delamination started at an applied displacement of 0.5 in. due to the reduction in stiffness at that point in time. It is also at this point that small cracks began forming on the underside of the precast panel.

Figure 5.2 Control specimen delamination at 1.2 in. of displacement. (Location: northwest)

Figure 5.3 Delamination at northwest corner of control specimen at 2.4 in. of displacement.

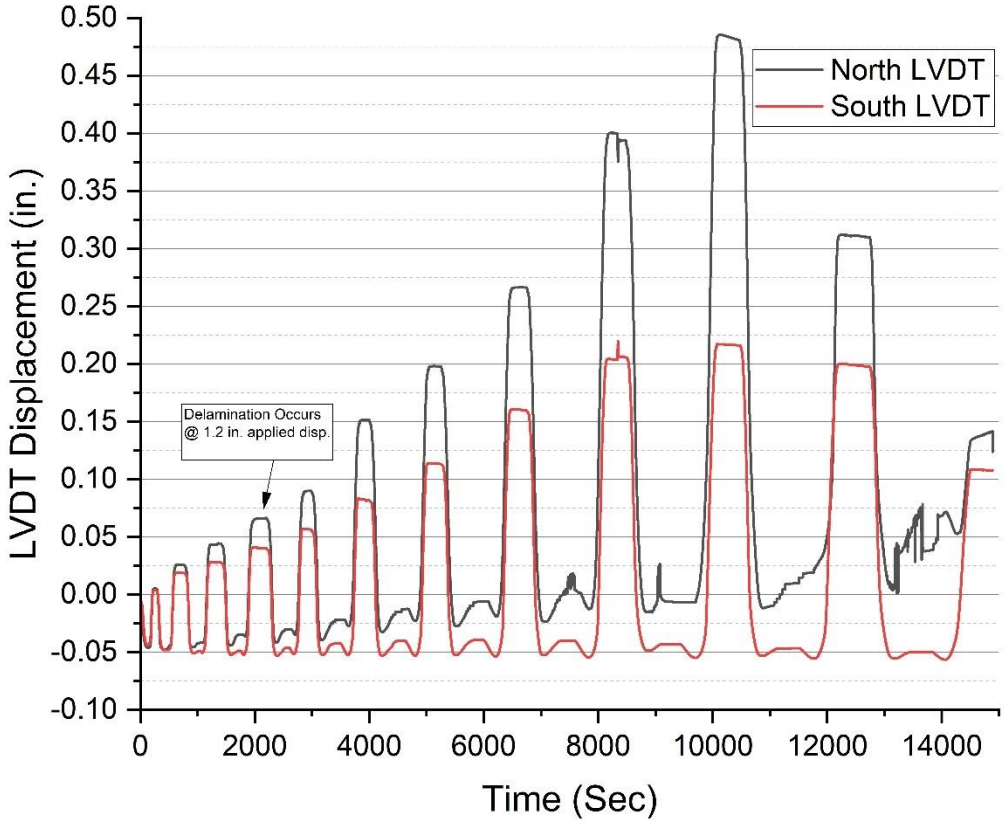

Figure 5.4 Test specimen with no retrofit (control) LVDT displacement at north and south.

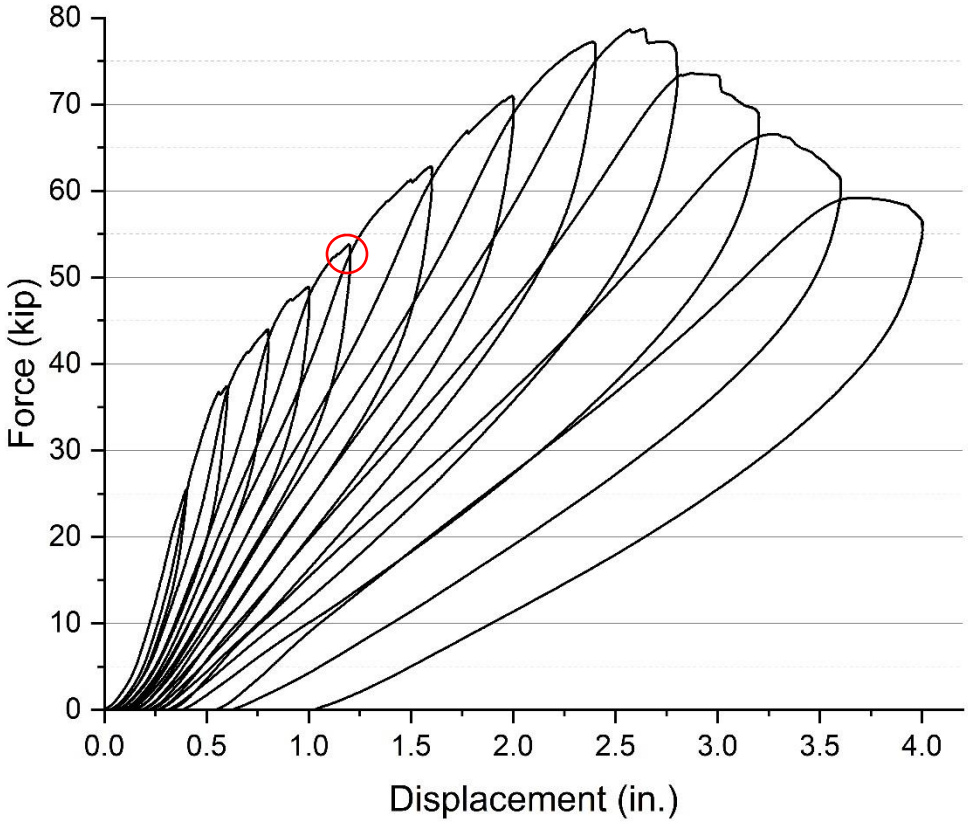

Figure 5.5 Test specimen with no retrofit (control) hysteresis with point of visible delamination circled in red.

5.2 Epoxy Injection

The deck panel with the epoxy injection retrofit resisted the displacement imposed by the hydraulic actuator until the epoxy bond between the precast section and CIP section of the panel failed. The initial delamination at the north and south extremes is shown in **Fig. 5.6**. The epoxy retrofit demonstrated perfectly composite behavior for the first cycle of 0.4 in. Once the epoxy bond had failed, the panel behaved almost identically to the panel without any retrofit from *Section 5.1*. Bond failure occurred at only the north side of the panel while the south end remained completely bonded; this type of failure created a large displacement in the north LVDT as shown in **Fig. 5.7**. The panel with epoxy bond was able to endure a maximum load of 63 kip before delamination, indicated in the hysteresis curves of **Fig. 5.8**. The precast and CIP sections of the panel continued to separate after the epoxy failure. **Fig. 5.9** demonstrates just how much the panel was able to separate; the gap measured almost 0.5 in. when the applied displacement was 4.0 in. During the test it was observed that the CIP section of the panel was deflecting laterally as shown in **Fig. 5.10**; this behavior was anticipated but the displacement was large.

Once the test had been stopped, the precast and CIP panels were removed and separated to verify the dispersion of the epoxy between the panel sections. **Fig. 5.11** shows that the epoxy had been able to fill the void between the two panels at each extreme; the figure also highlights the difficulty in injecting the epoxy in areas that do not have complete interlayer delamination.

With an approximate stiffness of 150 kip/in., the epoxy retrofit shows improvement over the unmodified panel's stiffness value of 63.3 kip/in. This information combined with the

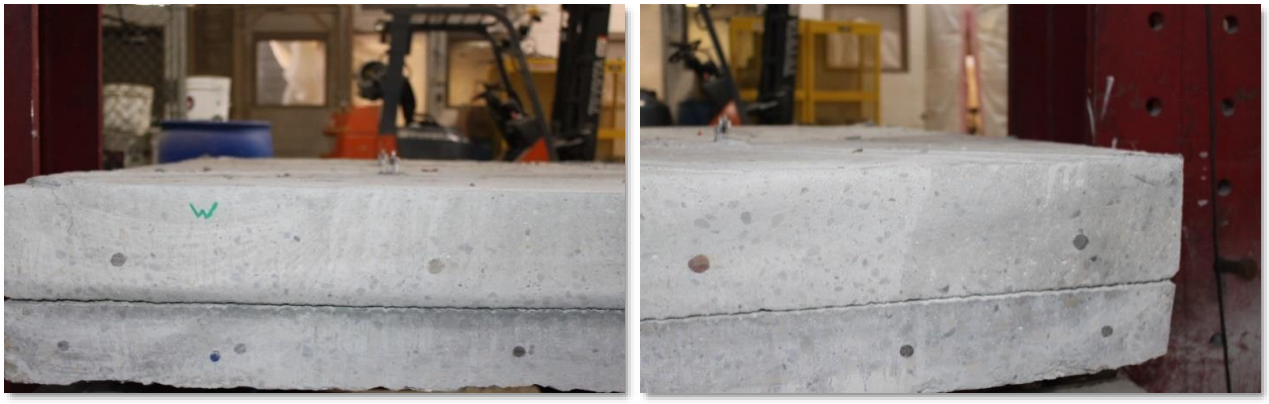

Figure 5.6 Epoxy retrofit initial delamination at northwest; left, southwest; right.

displacements recorded at the north and south extremes in **Fig. 5.7** indicates that the retrofit is successful until bond failure.

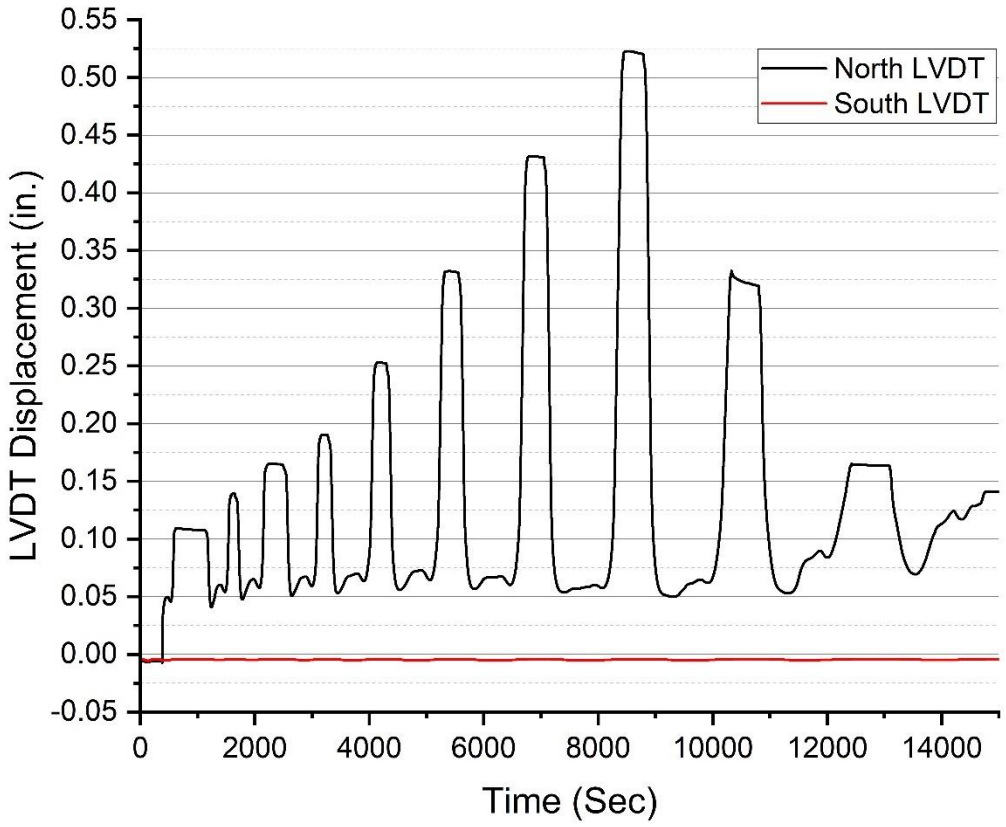

Figure 5.7 Epoxy retrofit panel LVDT displacement at north and south.

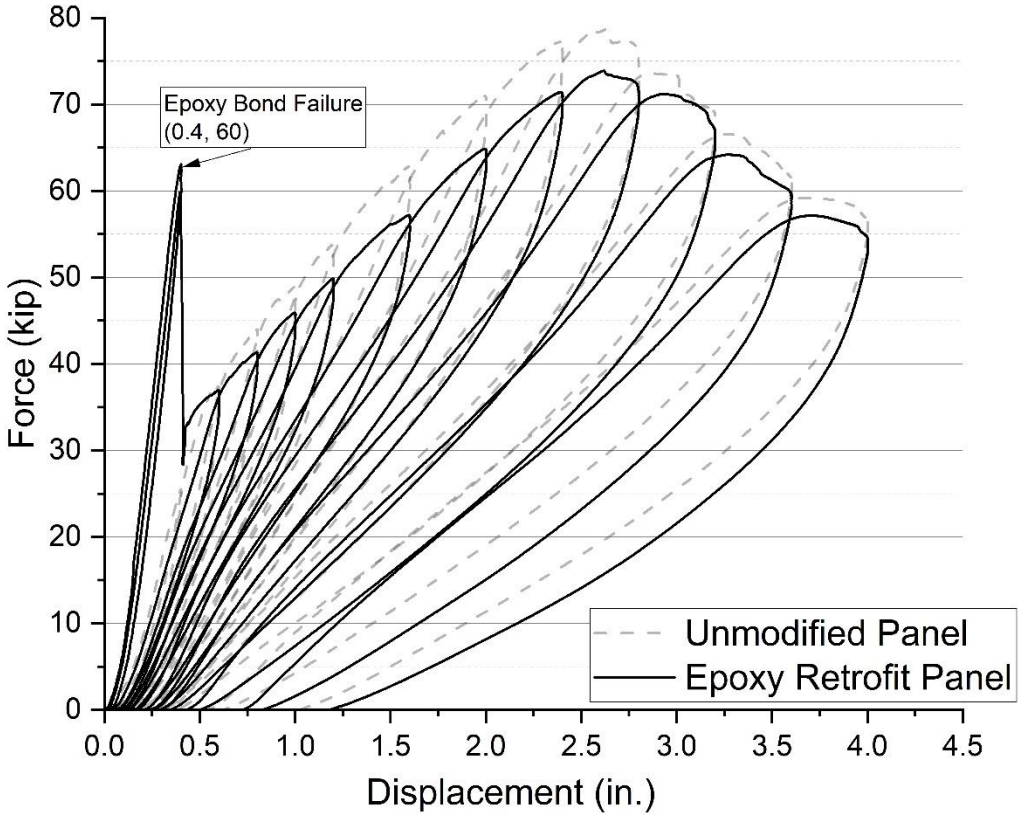

Figure 5.8 Epoxy retrofit panel hysteresis compared to the unmodified panel.

Figure 5.9 Delamination of epoxy retrofit deck panel at applied displacement of 4.0 in. (Location: northwest)

Figure 5.10 Lateral movement of epoxy retrofit deck panel at applied displacement of 4.0 in. (Location: northwest)

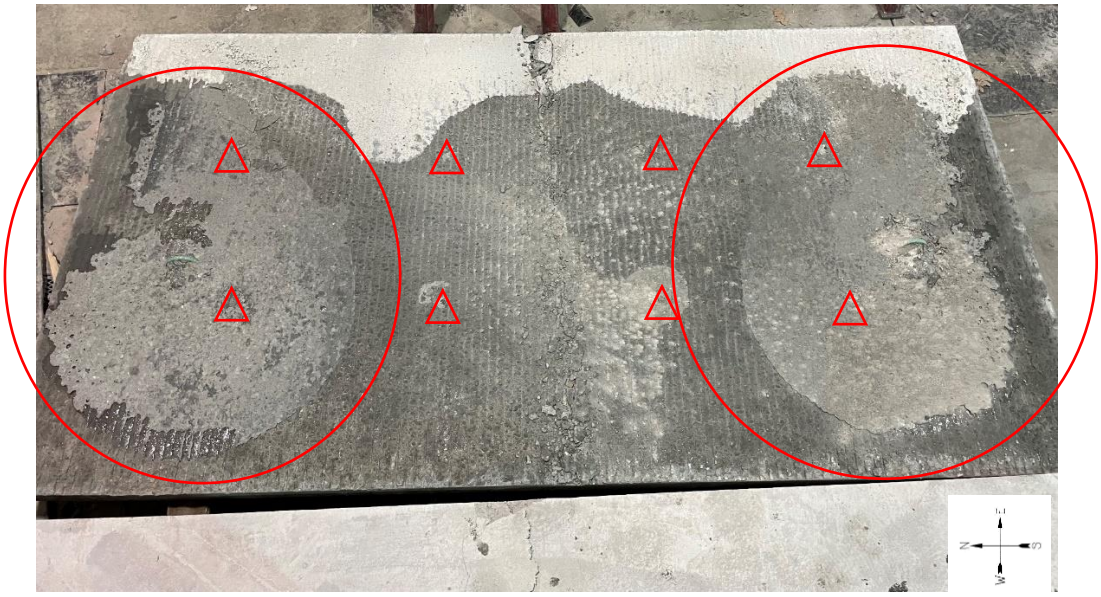

Figure 5.11 Distribution of epoxy after testing on the precast panel surface in plan view; triangles indicate location of epoxy injection sites.

5.3 Proprietary Mechanical Shear Anchors

The deck panel with the proprietary mechanical shear anchors had severe delamination prior to testing as shown in **Fig. 5.12**. In fact, the CIP section and precast section of the panel were entirely separate, which is a very extreme condition. The deck panel began to show evidence of cracking along the midspan at an applied displacement of 1.6 in., as shown in **Fig. 5.13**, but the delamination was restrained by the anchors and did not become critical.

With increased load, no delamination was observed, and the concrete of the CIP section of the panel began crushing at a displacement of 3.2 in., as shown in **Fig. 5.14**. Even with the concrete compression failure at the top surface of the panel, the proprietary mechanical shear anchors maintained composite action of the system.

Throughout the experiment, the deck panel retrofitted with shear anchors was able to keep interlayer delamination restrained within a tolerable range as indicated in **Fig. 5.15**. Another indicator of the shear anchor retrofit performance is deflection measured at midspan. **Fig. 5.16** shows that the panel was able to maintain its stiffness at large displacements, indicating that the

pre-cast and CIP sections of the panel behaved compositely after an initial slip. The panel with shear anchors was able to endure a maximum load of 76 kip and a displacement of 4.0 in.

The hysteresis curves indicate that the panel retrofitted with proprietary anchors was not the strongest panel tested but it was the best at resisting delamination. This panel was also the most compromised prior to testing, and it is believed that its ability to resist the applied load was reduced in part due to premature cracking.

Figure 5.12 Shear anchor retrofit deck panel initial delamination. (Location: left; southeast, right; northeast)

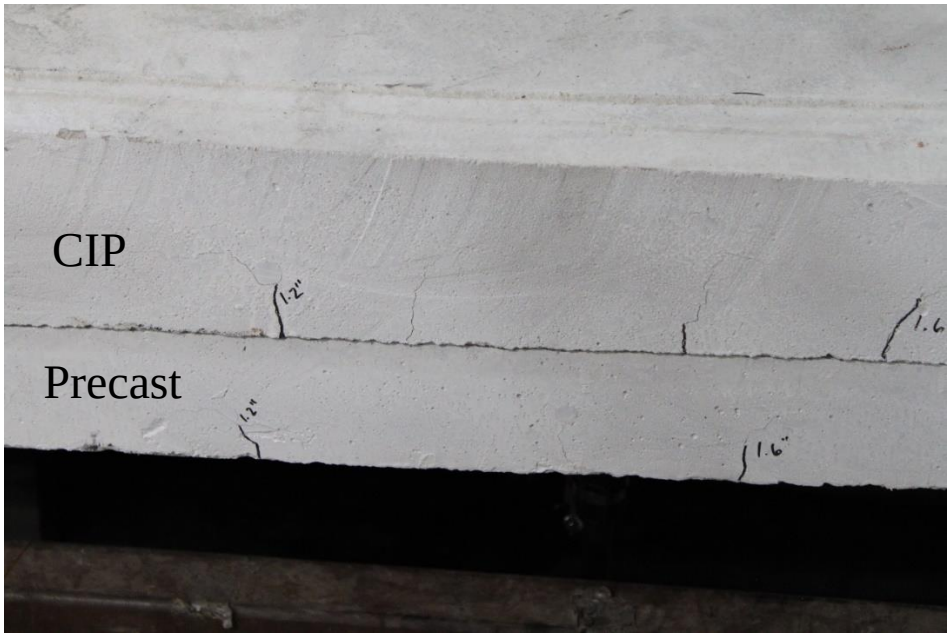

Figure 5.13 Shear anchor retrofit deck panel cracking after applied displacement of 1.6 in. (Location: east, mid-span)

Figure 5.14 Shear anchor retrofit deck panel compressive failure after applied displacement of 3.6 in. (Location: top, mid-span)

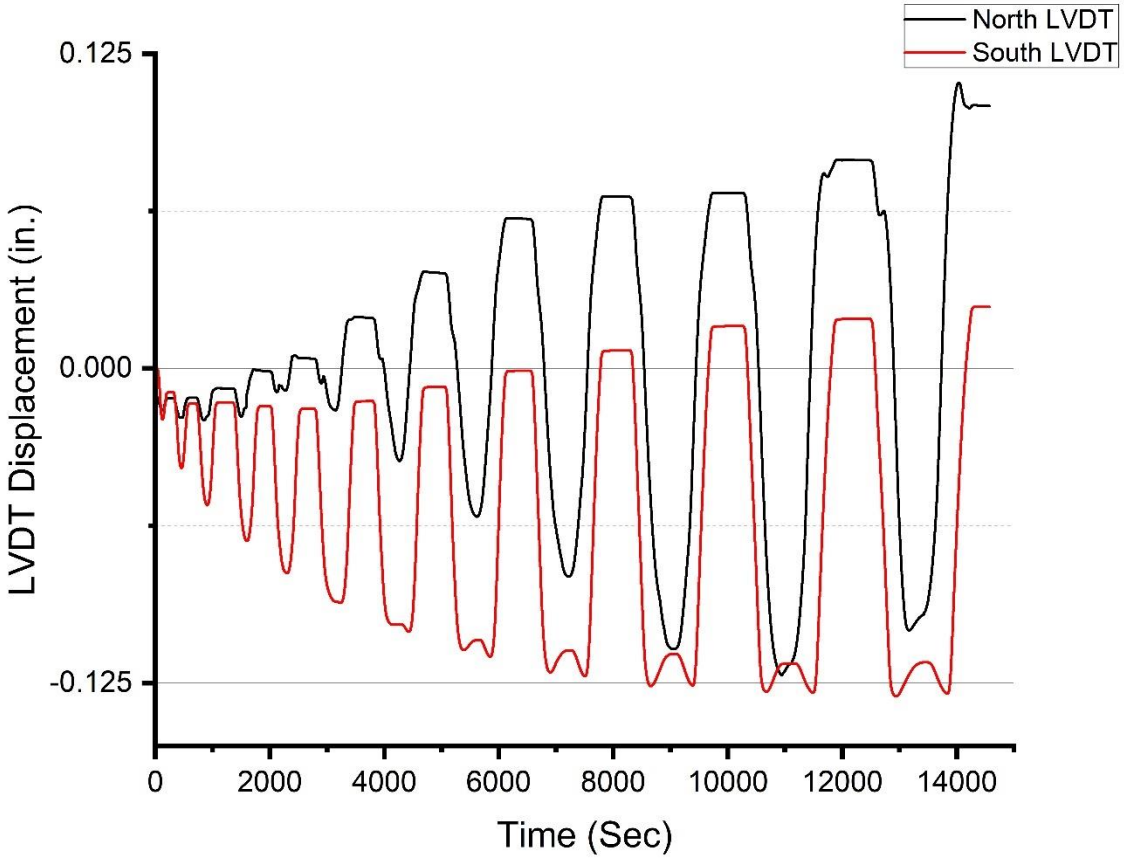

Figure 5.15 Shear anchor retrofit deck panel LVDT displacement at north and south.

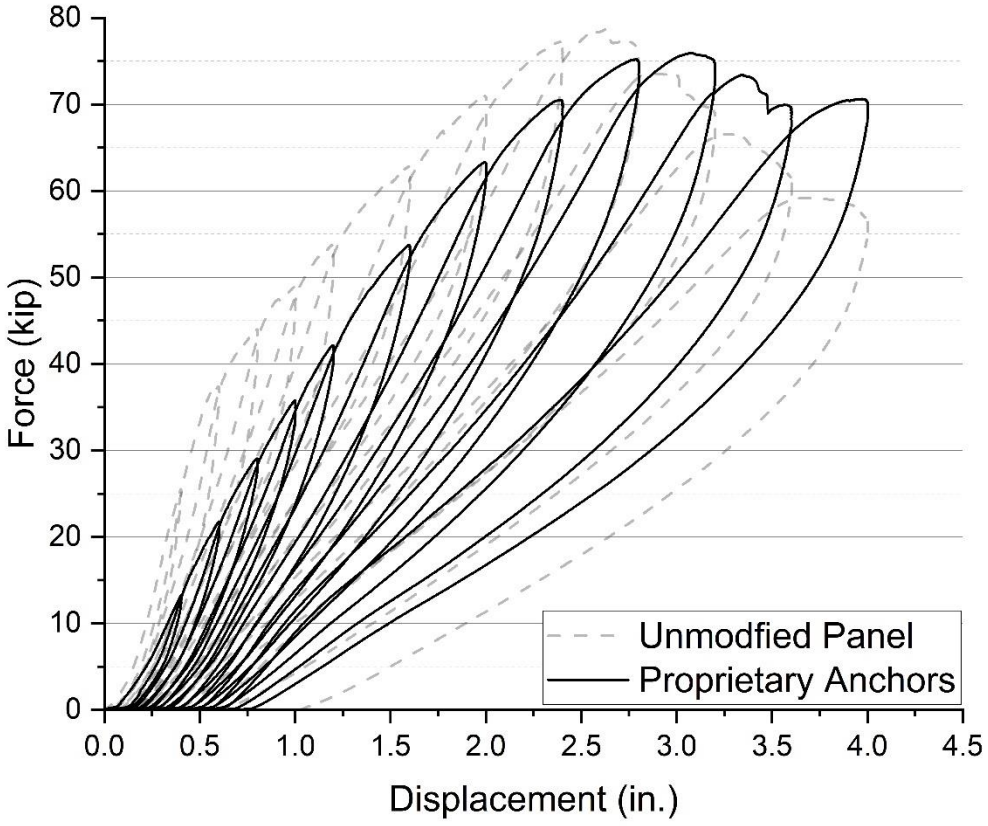

Figure 5.16 Shear anchor deck panel hysteresis.

5.4 Carbon Fiber Reinforced Polymer Strips

The deck panel specimen retrofitted with CFRP strips had an initial delamination of approximately 0.25 in., as shown in **Fig. 5.17**. At an applied 1.0-in. vertical displacement, the deck panel showed similar cracks to the control panel along the face of the CIP section of concrete, as shown in **Fig. 5.18**. At a 2.0-in. applied displacement, flexural cracks became visible in the precast panel as seen in **Fig. 5.19**. The test panel performed similarly to the unmodified specimen until a displacement of 1.2 in. At that point, tension in the CFRP strips had become large enough to resist further deflection at midspan. However, the additional strength provided by the CFRP was not sufficient to eliminate delamination. The CFRP strips did not fracture but, as **Fig. 5.20** shows, the CFRP strips debonded from the precast panel. **Fig. 5.21** shows that the north and south LVDTs were recording significantly different displacements, indicating delamination is occurring. Even with the additional flexural benefits provided by the CFRP strips, the specimen could not resist delamination in the presence of the increased horizontal shear forces.

At 2.4 in. of applied displacement, the bond of the CFRP strips to the precast panel had deteriorated and this bond could no longer support additional deflection. The failure was catastrophic and is shown by the sharp drop in load in **Fig. 5.22**. The CFRP retrofitted panel behaved similarly to the unmodified panel except for the increased strength, as shown in **Fig. 5.23**.

Figure 5.17 CFRP retrofit deck panel initial delamination prior to testing. (Location: southeast corner)

Figure 5.18 CFRP retrofit deck panel cracks at 1.0-in. displacement. (Location: east, mid-span)

Figure 5.19 CFRP retrofit deck delamination at 2.0-in. displacement (Location: east, mid-span)

Figure 5.20 East CFRP bond failure at applied displacement of 2.4 in.

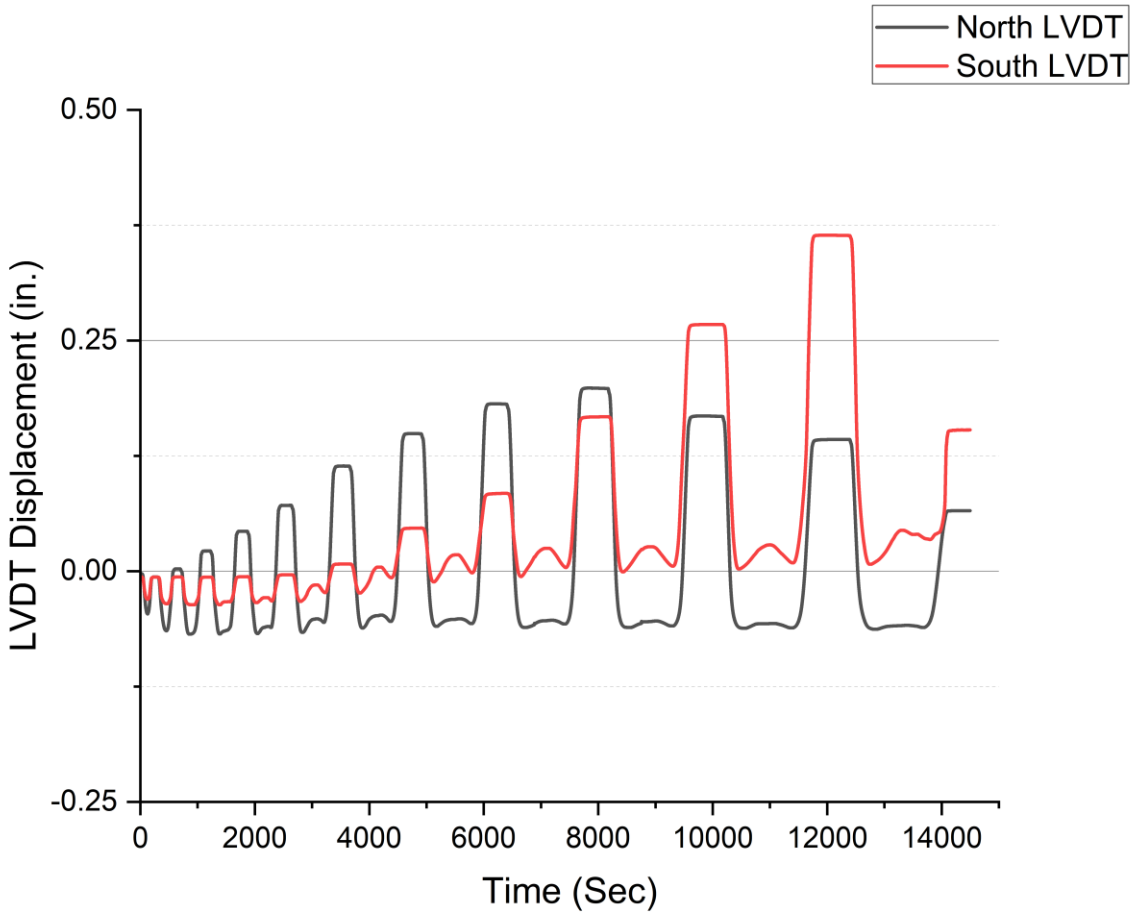

Figure 5.21 CFRP retrofit LVDT displacement at north and south.

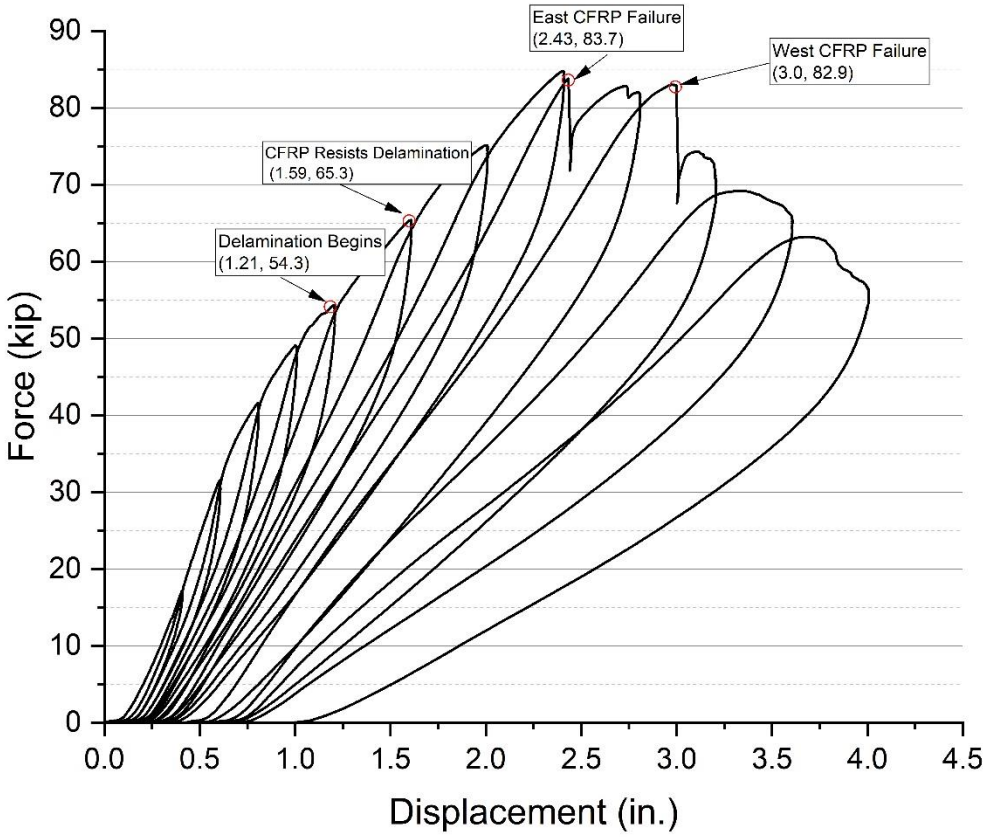

Figure 5.22 CFRP retrofit deck panel hysteresis with points of interest.

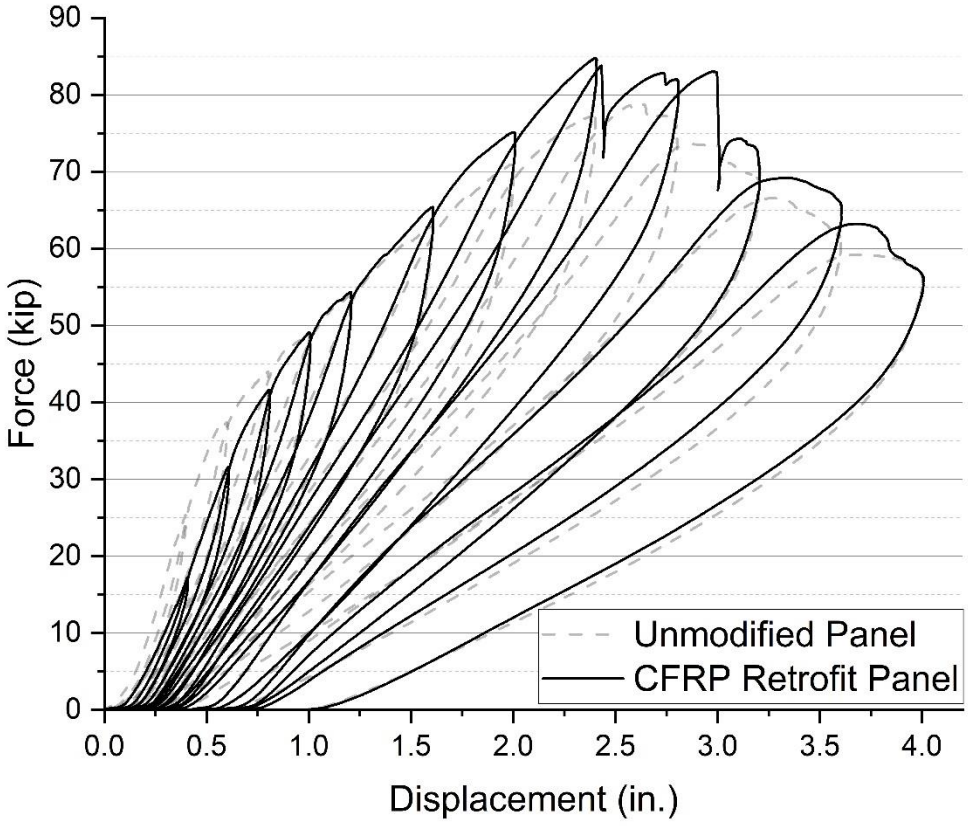

Figure 5.23 CFRP retrofitted and unmodified panel comparison.

5.5 Nonproprietary Shear Anchors

The nonproprietary shear anchors performed almost identically to the mechanical shear anchors discussed in *Section 5.3*. Small flexural cracking began at 1.6 in. of displacement at the mid span of the panel indicated by the red circles in **Fig. 5.24**. Even at 2.0 in. of applied displacement, the shear slip at the north and south extremes between the two panels was negligible as shown in **Fig. 5.25**. After the test, the panel was inverted and evaluated revealing significant cracking along the underside of the panel. No failure of the tendons was observed in the precast panel. The primary failure mode for this specimen was the crushing failure at the top CIP section. **Fig. 5.26** shows the test panel inverted, and the red circles indicate anchor locations.

Fig. 5.27 shows the hysteresis of the panel with nonproprietary anchors, and **Fig. 5.28** shows a comparison of hysteresis curves for the nonproprietary and proprietary anchors. Even though the panel fitted with the proprietary anchors was the most compromised panel, the anchors were able to improve the performance similar to the nonproprietary shear anchors.

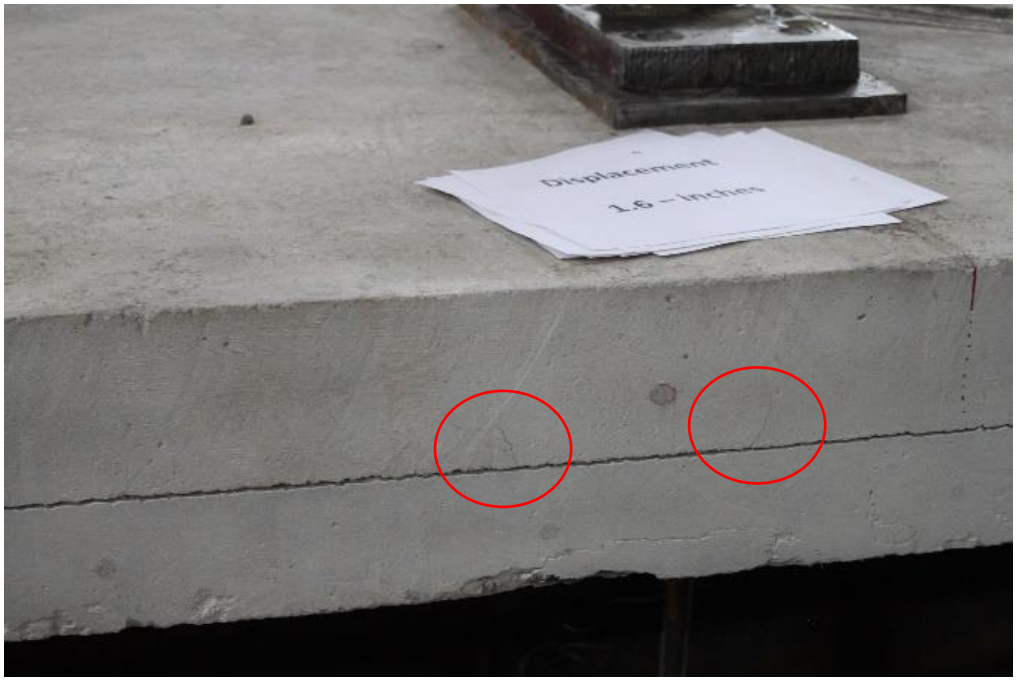

Figure 5.24 Flexural cracks at 1.6 in. of displacement.

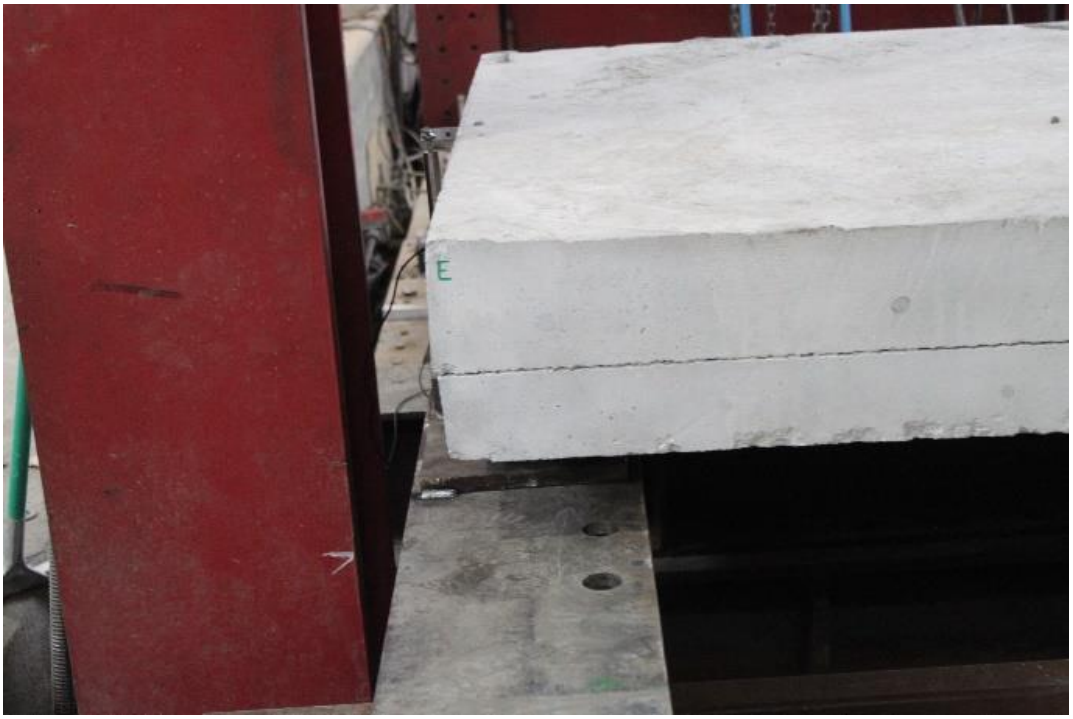

Figure 5.25 CIP and precast deck panel at 2.0 in. of displacement. (Location: southeast).

Figure 5.26 Test panel with nonproprietary anchor retrofit. The test panel is inverted, the red circles indicate the locations of the anchors.

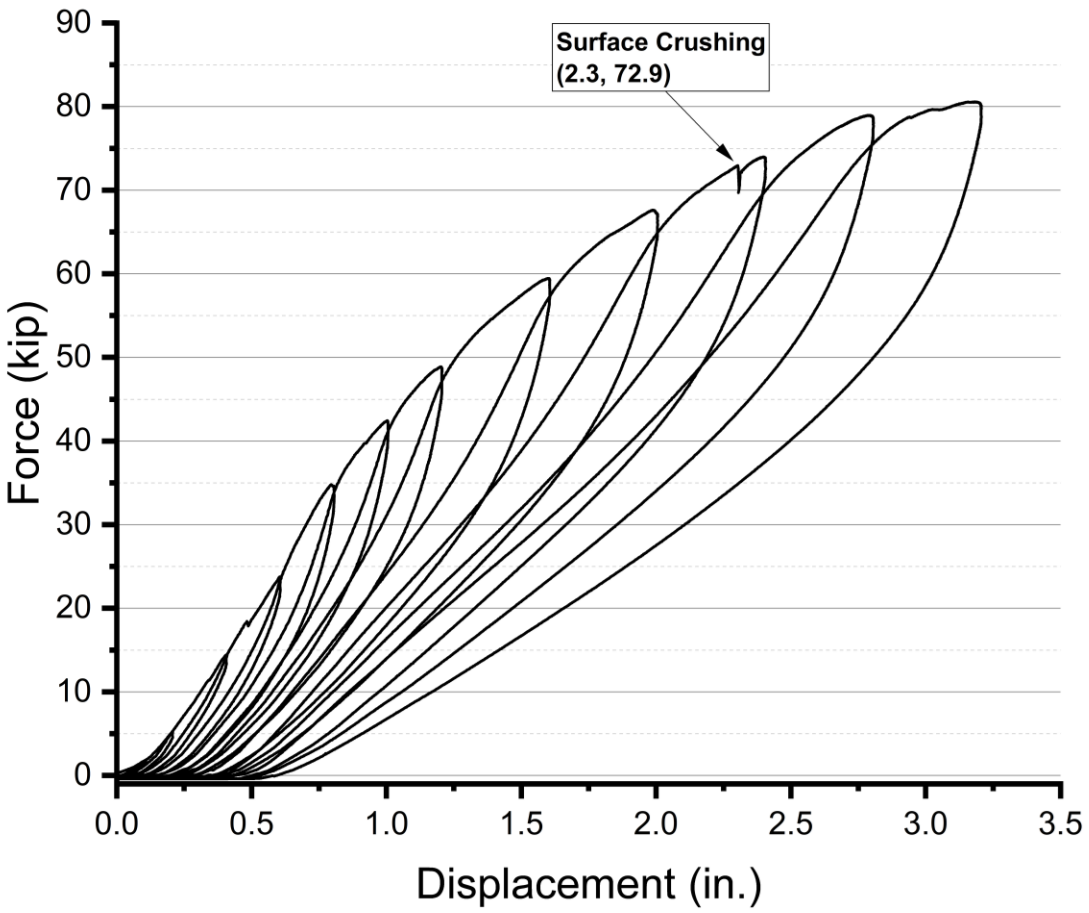

Figure 5.27 Nonproprietary shear anchor hysteresis.

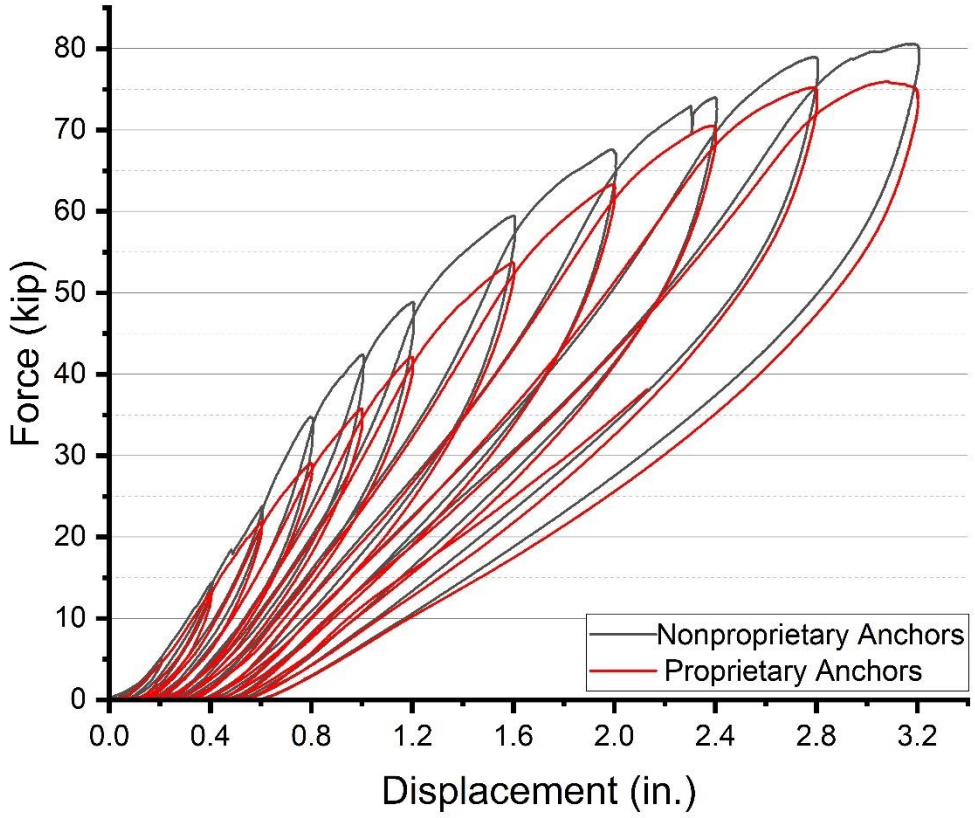

Figure 5.28 Nonproprietary shear anchors' hysteresis compared to proprietary shear anchor hysteresis.

5.6 Proprietary Mechanical Shear Anchors with Epoxy Injection

The epoxy injection filled the void between the CIP and PC panels and can be observed in **Fig. 5.29.** Small flexural cracking occurred after the 0.6-in. loading cycle, as shown in **Fig. 5.30**, with no observable drop in the load. The epoxy injection improved the composite behavior of the panel until bond failure at a displacement of 0.78 in. and a force of 67.8 kip. Similar to the previously tested panel with epoxy retrofit, the epoxy bond failed at one end of the panel only. **Fig. 5.31** shows just how severe the delamination can be under extreme conditions. The hysteresis in **Fig. 5.32** highlights this dramatic improvement in the panel's stiffness up to the point of bond failure. After the epoxy bond failed, the anchors resisted the load and maintained the composite behavior of the panel until surface crushing failure occurred. Unlike the panel that was only retrofitted with epoxy injection, the panel with anchors was able to resist the additional load by restraining the sudden release of energy and sudden load drop resulting from bond failure that was observed for the panel with epoxy injection, as shown in **Fig. 5.33**.

Figure 5.29 Epoxy injection with proprietary shear anchors before loading.

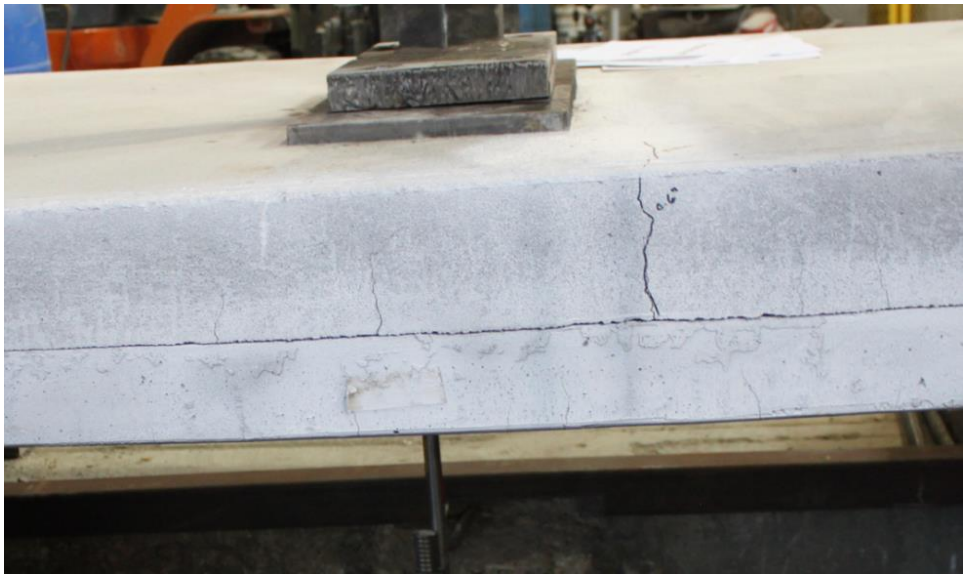

Figure 5.30 Flexural cracking at midspan.

Figure 5.31 Delamination of CIP and PC decks at 1.6 in. of applied displacement. (Location: southeast).

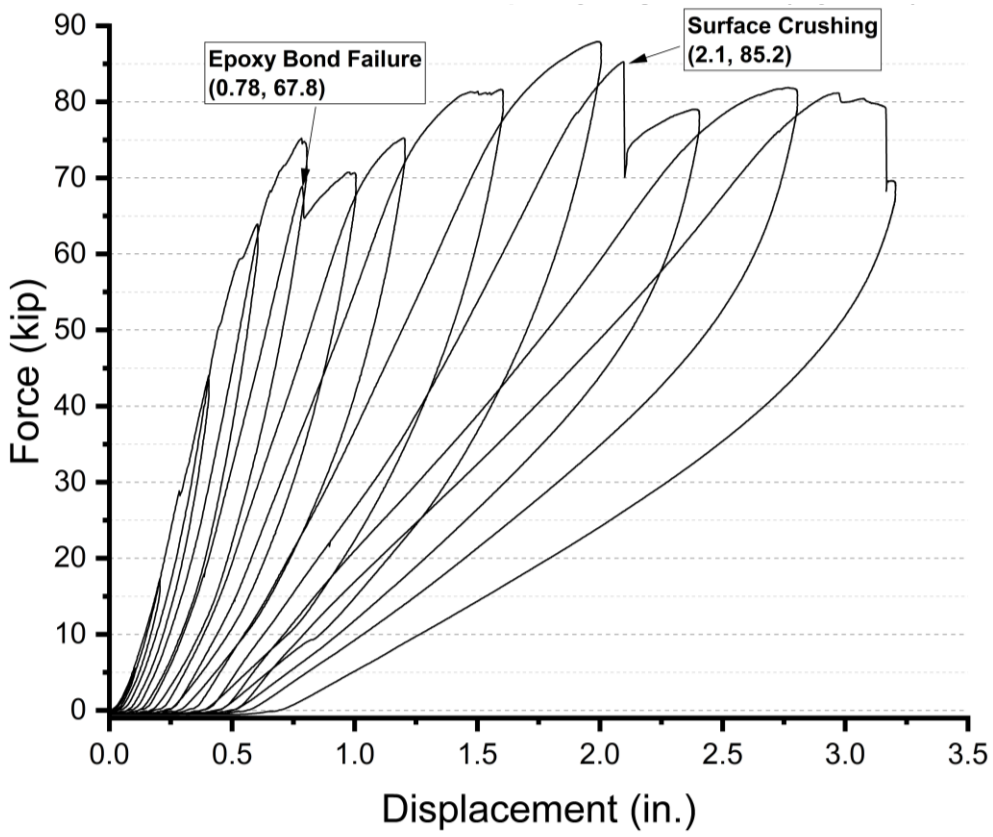

Figure 5.32 Epoxy injection with proprietary shear anchor hysteresis.

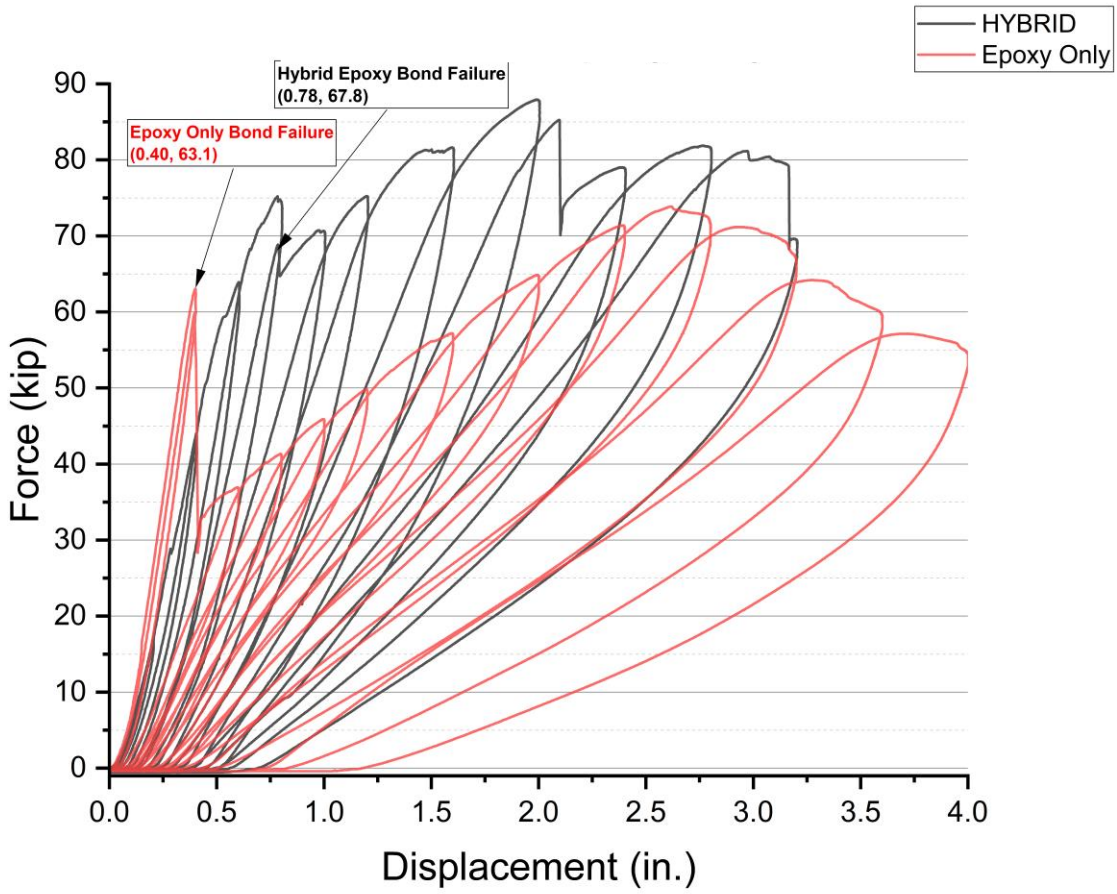

Figure 5.33 Epoxy injection with proprietary shear anchor retrofit compared to the epoxy injection only retrofit.

5.7 Comparison of Retrofit Methods

The five retrofit methods are compared by plotting the hysteresis envelopes in **Fig. 5.34.** The peak force values at the applied displacement cycle allow for quick analysis of all five specimens. The two specimens that were retrofitted using the epoxy injection method show an increased stiffness and a significant improvement in overall strength. Outside of the two test specimens retrofitted with epoxy injection, the remaining panels followed a similar trend. The panel treated with just the epoxy injection retrofit follows this trend after the epoxy bond breaks.

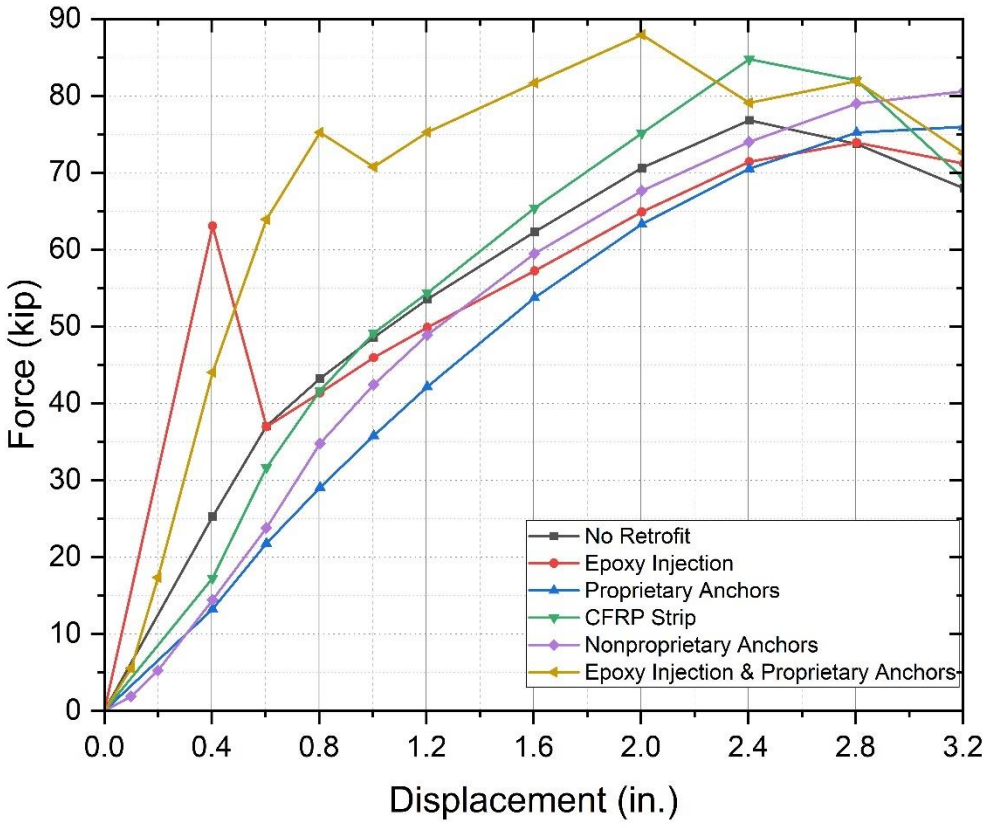

Figure 5.34 Peak force comparison of the five retrofit methods.

6 SALVAGED PANELS

6.1 Salvaged Panel Overview

UDOT provided the research team with two salvaged panels for testing. These panels were cut from the 800 South bridge on Interstate 15 in Salt Lake City. The original location of the panels is indicated in **Fig. 6.1**. **Fig. 6.2** shows the panels that were removed from the bridge. For this report the salvaged panel that was taken from the HOV lane will be referred to as P-A, and the second salvaged panel taken from the east cut site will be referred to as P-B.

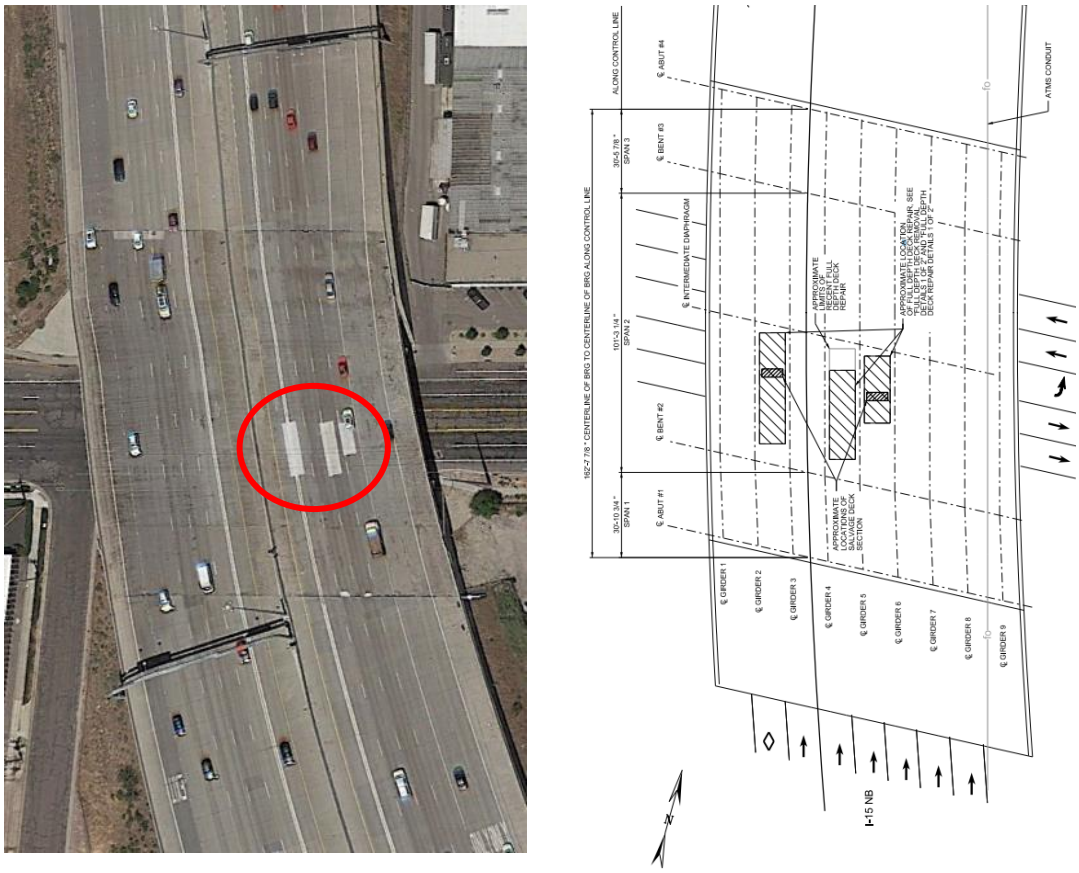

Figure 6.1 Location of salvaged panel cuts.

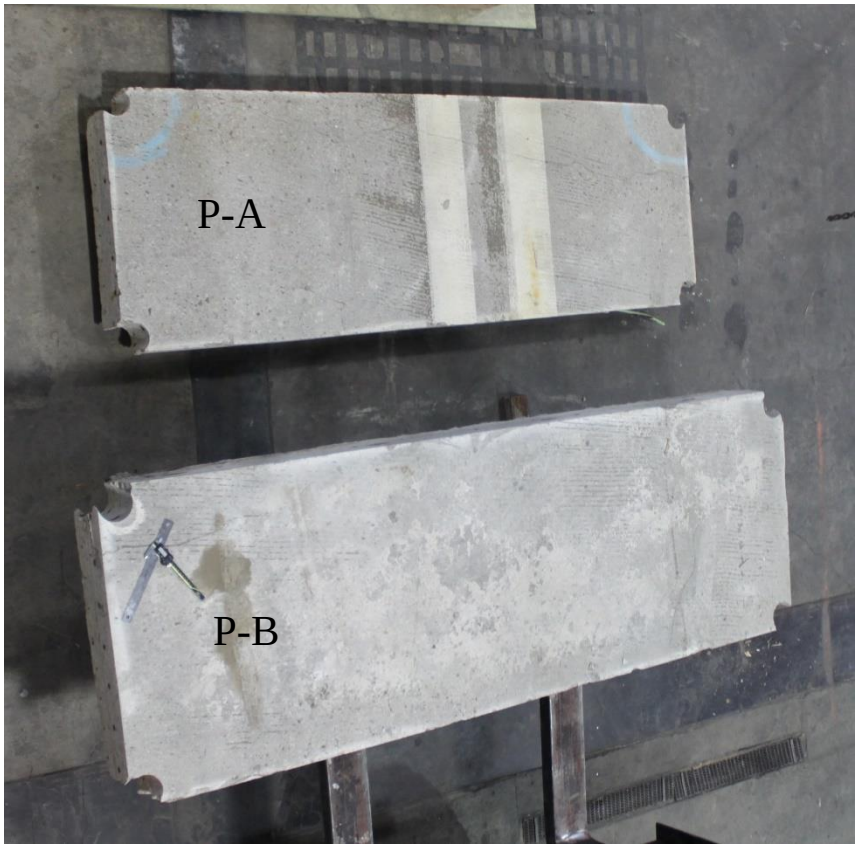

Figure 6.2 Salvaged specimen overview.

Initial inspection of the salvaged panels indicated that panel P-B had severe delamination between the cast-in-place and precast deck sections (**Fig. 6.3**). Panel P-A did not have the same delamination and appeared to be intact (**Fig. 6.4**). No abnormalities in the precast panel were observed, and the CIP decks of both panels appeared to be intact without any significant cracking.

Figure 6.3 Comparison of salvaged panels.

Figure 6.4 Salvaged panel comparison of delamination.

Panels P-A and P-B were both cut to fit within the confines of the testing fixture. The specimens were reduced in size to 7ft – 8in. with a clear span of 87 in. The salvaged panels were identical to the test specimens created with the exception of the transverse direction; the salvaged test specimens measured 3ft-0 in. in this direction. This cut also revealed that the CIP deck of

panel P-B had not bonded to the precast deck at all (**Fig. 6.5**). Separating the CIP deck from the precast deck of the cut section also revealed a chalky substance indicating a possible surface contaminant.

Figure 6.5 Cut section of P-B separated exposing mating interface between panels.

6.2 Salvaged Panel with No Retrofit (P-A)

Panel P-A was selected as the salvaged panel that would not be retrofitted due to its composite appearance. **Fig. 6.6** shows that the initial gap between the CIP deck and precast sections is effectively zero. At a displacement of 0.8 in., panel P-A began to show the formation of flexural cracks measuring 0.02 in. at midspan (**Fig. 6.7**). At 1.2-in. displacement, the CIP and precast sections began to separate only at the region centered at midspan, as shown in **Fig. 6.8.**

Figure 6.6 Salvaged panel with no visible delamination. (Location: southeast)

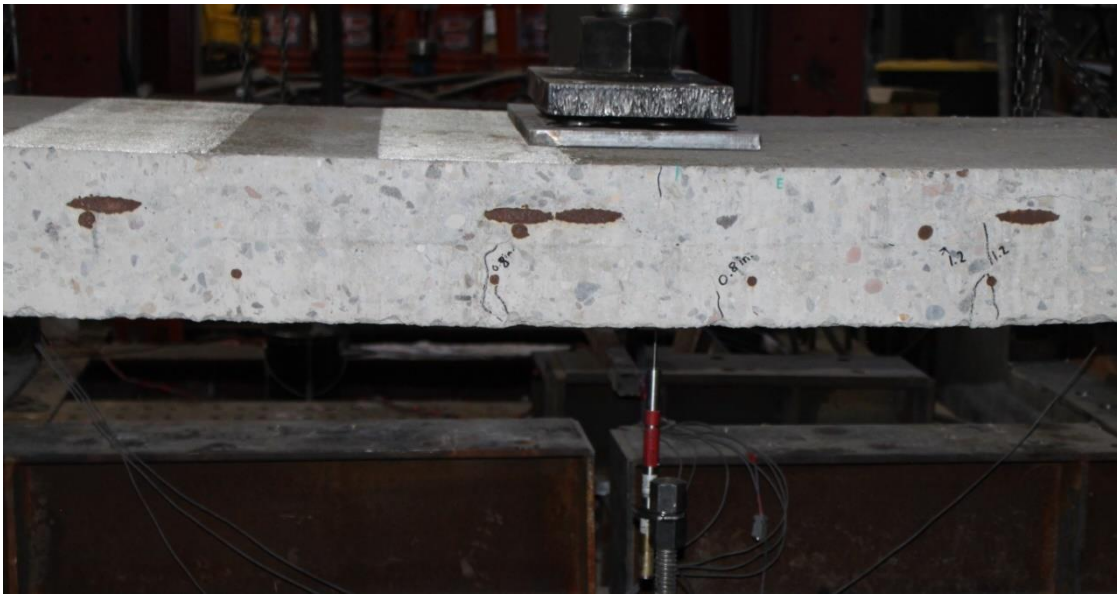

Figure 6.7 Salvaged panel flexural cracking at midspan.

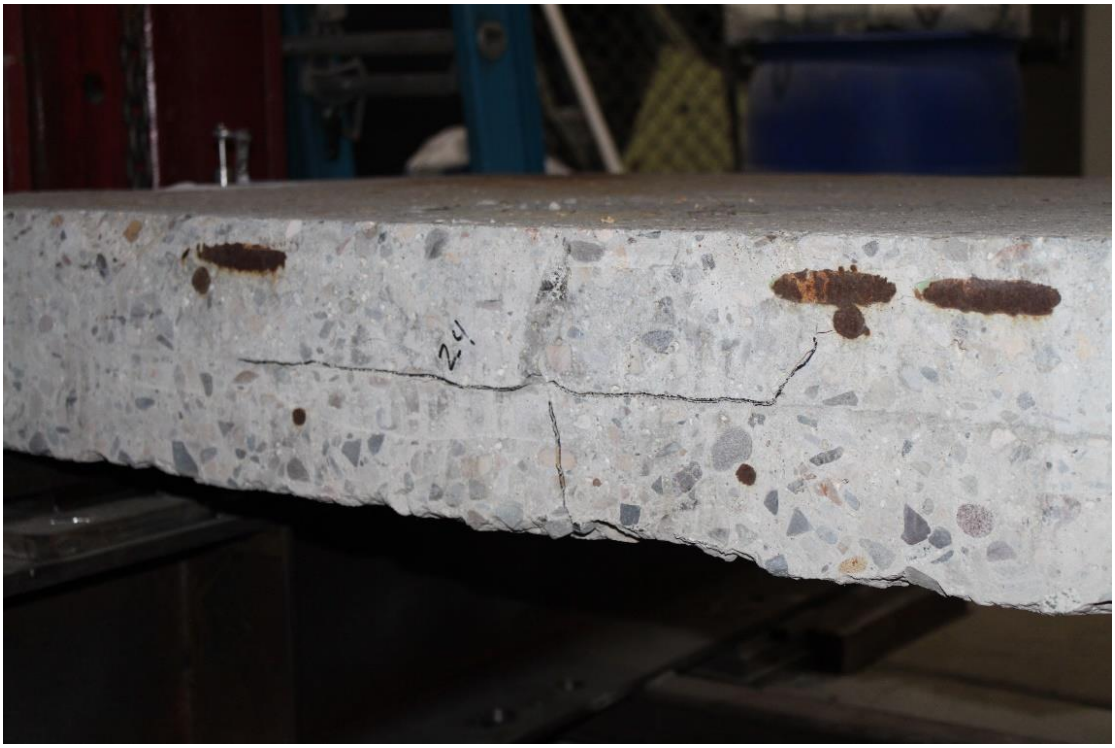

Figure 6.8 Salvaged panel with no retrofit delamination after 2.4 in. of applied displacement.

With the observations made during the test, it was clear that this salvaged panel with no retrofit was in fact behaving compositely. Analysis of the hysteresis curves in **Fig. 6.9** revealed a high initial stiffness until 0.4 in. where a small drop in force resulted; this drop could have been from internal delamination of the sections, but it was not immediately evident from the exterior. With this information, it was concluded that panel P-A before testing was practically in a composite condition.

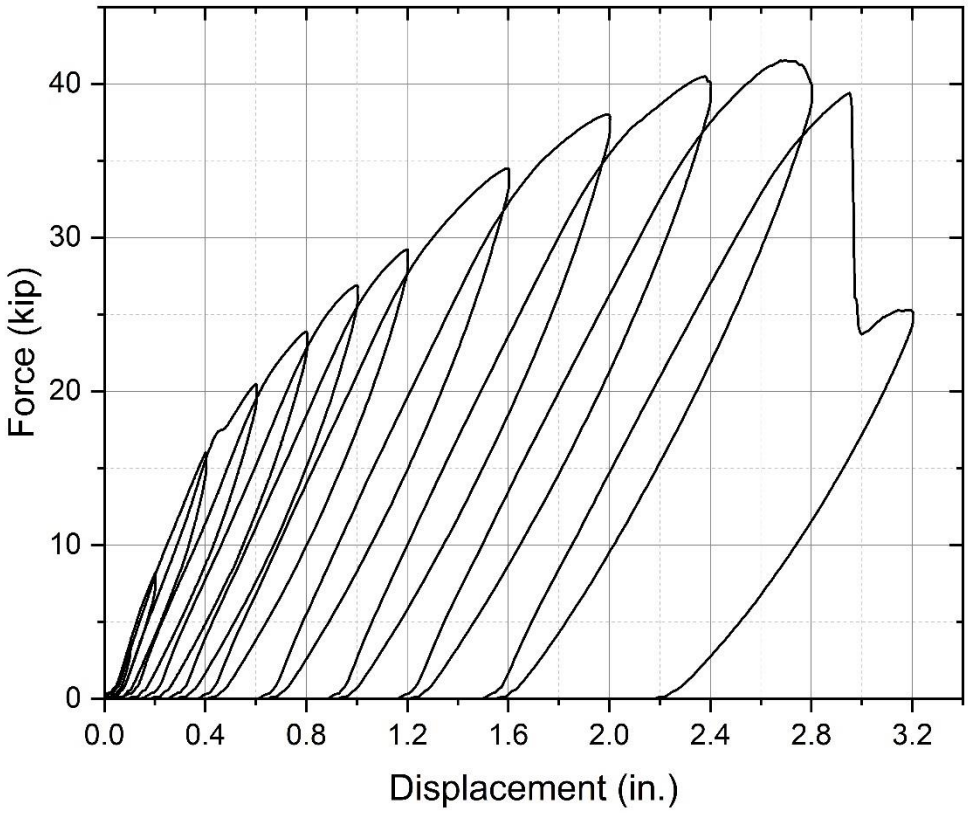

Figure 6.9 Salvaged panel with no retrofit hysteresis curve.

6.3 Salvaged Panel with Epoxy Injection Retrofit (P-B)

Panel P-B was severely delaminated prior to testing and as a result was selected for the epoxy injection retrofit. The epoxy was injected into ports spaced at the same distance as the panel from *Section 3.1*, as shown in **Fig. 6.10**. To restrict the epoxy to stay within the confines of the panel, the outside face of panel P-B was sealed with a thin layer of red adhesive (**Fig. 6.11**). Approximately 0.75 gallons of epoxy (3 tubes) was injected into the panel. Epoxy was observed filling many of the small cracks of the panel. It should be noted that no preparations were made to remove the contamination between the precast and cast-in-place sections.

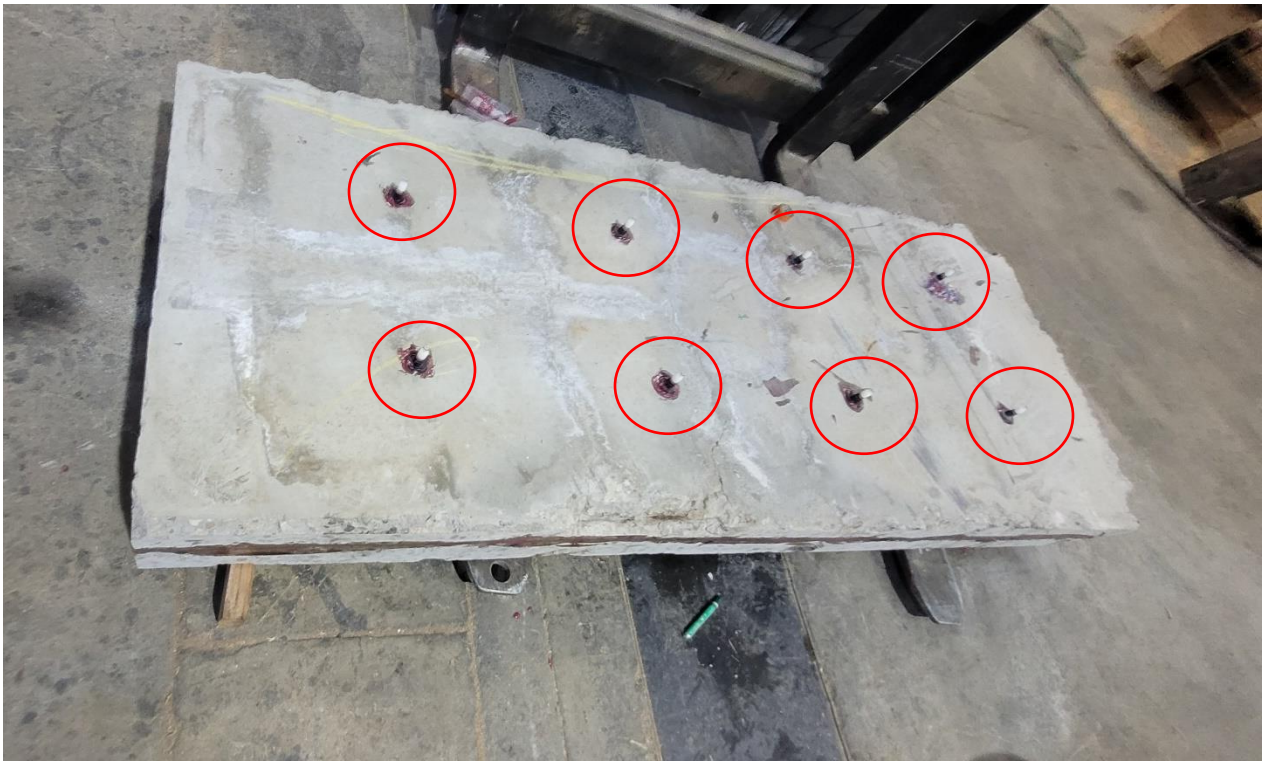

Figure 6.10 Inverted salvaged test panel with epoxy injection ports highlighted in red.

Figure 6.11 Salvaged panel being injected with epoxy.

Panel P-B was tested using the second loading protocol that was developed and is outlined in *Section 4.2*. Similar to other tests, small flexural cracks appeared at midspan. No observable delamination was recorded at the north and south extremes until epoxy bond failure. The epoxy failed at the south end of the panel, as shown in **Fig. 6.12**. Failure occurred at 2.5 in. of applied displacement and 45.3 kip force. The hysteresis curve in **Fig. 6.13** indicates that no significant drop in panel stiffness occurred until 1.2 in. of applied displacement.

Figure 6.12 Epoxy bond failure of P-B after 2.5 in. of applied displacement. (Location: southeast)

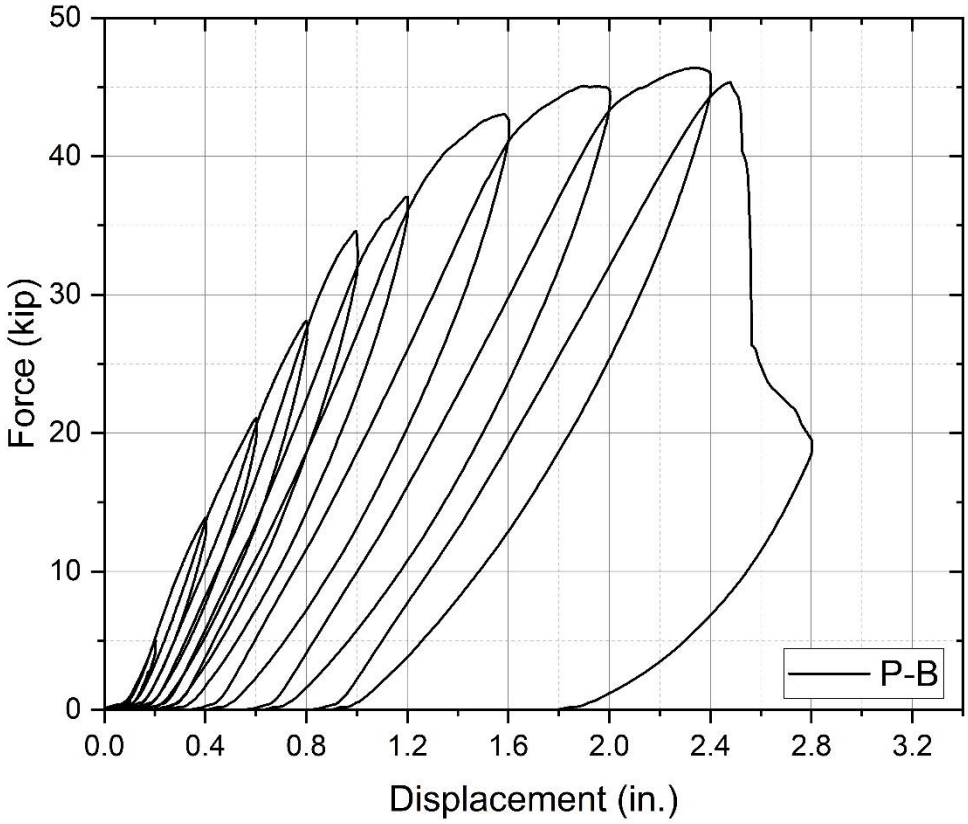

Figure 6.13 Hysteresis curve of P-B.

6.4 Comparison of Salvaged Panels

The hysteresis curves of the two salvaged test panels were compared (see **Fig. 6.14**). The epoxy retrofitted panel, P-B in red, showed significant improvement in stiffness and strength compared to panel, P-A in black, without any retrofit. Panel P-A is not a fully composite panel but since it delaminated well after the allowable deflection of span/300 (0.3 in.), its performance is better than a fully delaminated panel.

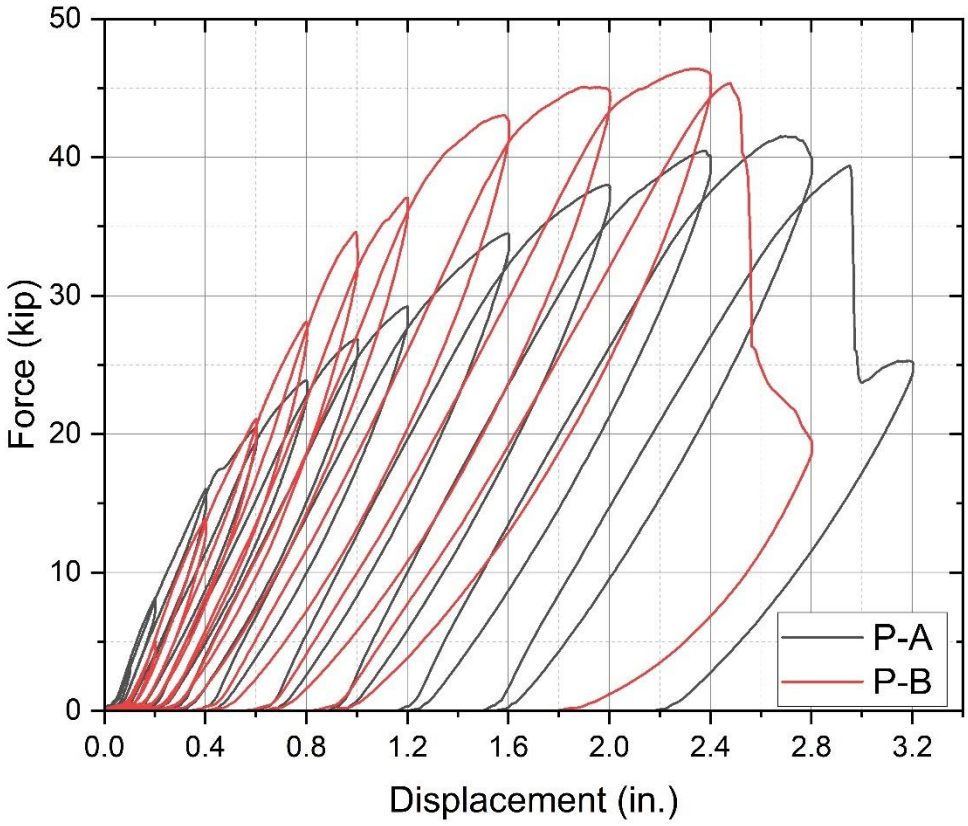

Figure 6.14 Hysteresis comparison of P-A to P-B. (P-A: salvaged panel with no retrofit, P-B: salvaged panel with epoxy injection retrofit)

7 NUMERICAL MODEL

7.1 Material Properties

7.1.1 Concrete Damage Plasticity Model

A reliable technique for modeling the nonlinearity of concrete in structural analysis is the concrete damage plasticity (CDP) model, which is integrated into ABAQUS (Simulia, 2019). It accurately illustrates the relationship between stress and strain in concrete under various loading conditions by combining the material's plasticity and isotropic damage elasticity. This model is beneficial for modeling the response of concrete structures under different load conditions because it captures significant phenomena such as strain-softening and tension-stiffening. CDP can simulate both tensile cracking and compressive crushing as a failure mode (Lee and Fenves, 1998). The overall reliability of structural analysis has been improved by the successful prediction of the failure processes and structural response of concrete elements using the CDP model in numerical analysis. The CDP model for this analysis was generated for concrete with a compressive strength of 8 ksi and used for modeling. The precast panel was aged and was assumed to have a compressive strength of 8 ksi; the cast in-place was lower than this, but the FEM model required a higher compressive strength to replicate the experimental results. **Fig. 7.1** shows the material properties of the CDP material used in the FEM modeling of the bridge decks. **Table 7.1** shows the plasticity parameters used in the ABAQUS model to simulate actual behavior of concrete.

Table 7.1 CDP material properties

Dilation angle	Eccentricity	Fb0/fc0	K
35	0.1	1.16	0.667

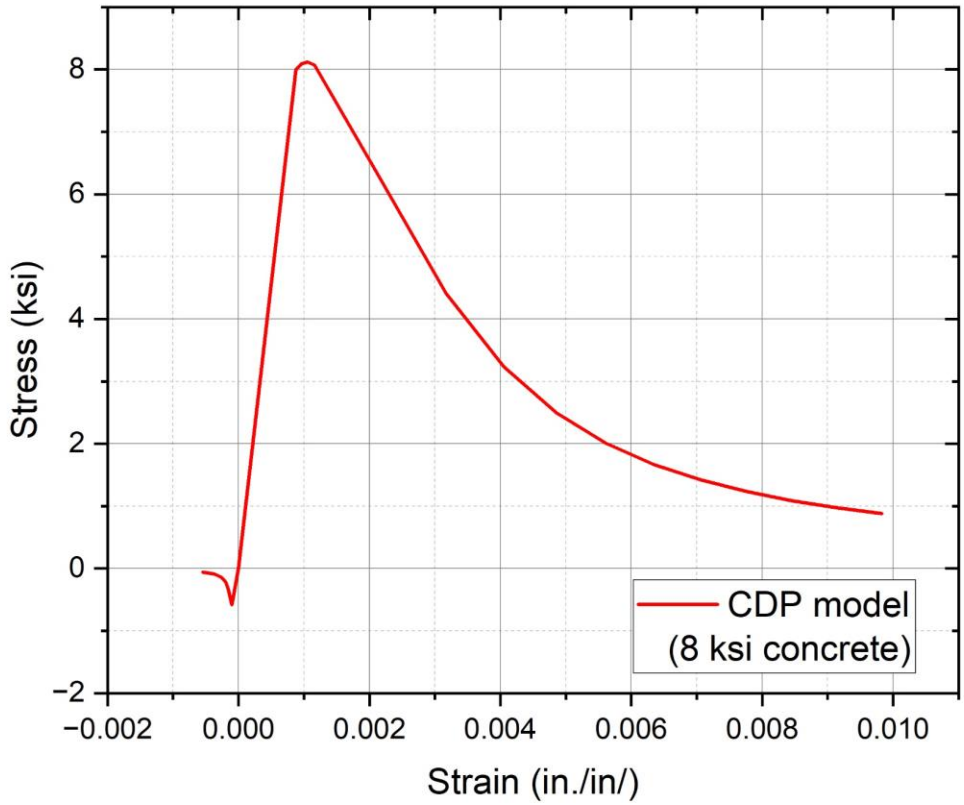

Figure 7.1 Concrete damage plasticity model material properties.

7.1.2 Steel Reinforcement and Prestressed Steel Tendon Material Properties

In the experimental study, ASTM A615 Grade 60 steel reinforcing bars were used, and the standard specified properties of these bars were used to model them within the finite element analysis. The reinforcing bars were represented as truss elements, incorporating the properties of the steel reinforcement. The specific reinforcing bars had a yield strength of 68 ksi and an ultimate strength of 99 ksi. The stress-strain curve for the reinforcing bars used in the finite element model is shown in **Fig 7.2(a)**. This curve shows the typical behavior of Grade 60 steel reinforcing bars under the applied loading conditions, serving as a fundamental component in the accurate representation of the bars' response within the finite element model. Prestressed tendons

are used in the long axis of the precast slab. The finite element model in ABAQUS incorporates the physical non-linear characteristics of the 7-wire strand tendons in the numerical model, and an initial predefined stress is applied to replicate the initial prestress in the tendons. The material properties of the prestressed tendons used in the finite element model are shown in **Fig. 7.2(b)**.

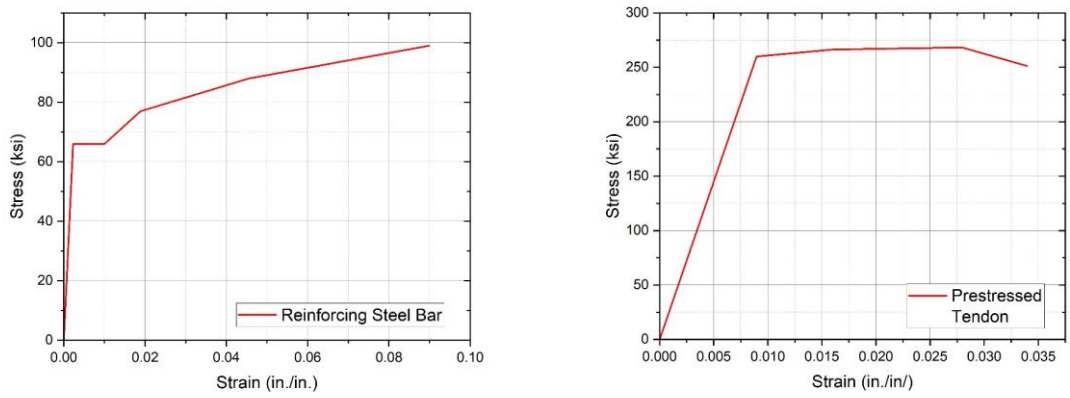

(a) (b)

Figure 7.2 Steel reinforcement material properties: (a) steel reinforcing bars; (b) prestressed tendons.

7.2 Model Layout

Two different deck panels were modeled in ABAQUS. The CDP material properties are included in the FEM model to represent both tensile and compressive failure within the concrete. Both panel sections are modeled as a C3D8R solid brick element type. A 0.5-inch-thick steel plate was used to distribute the load; this loading plate was tied together with the concrete surface on the CIP section. A reference point was created and coupled to the top surface of the loading plate simulating the load distribution of the actuator during the experiment. The loading plate was modeled as a solid C3D8R brick element. D-shaped elastic supports were modeled as supports to simulate the simply supported connection during the experiment and modeled as solid C3D8R brick elements. Boundary conditions are applied to represent the experimental setup. The D-shaped steel support was modeled as an elastic material and only general friction with a frictional coefficient 0.45 in the tangential direction, and hard contact in the normal direction was used to simulate the

interaction between supports and bottom slab surface. **Fig. 7.3** shows the experimental setup with the supports and actuator load application in the loading plate using reference point.

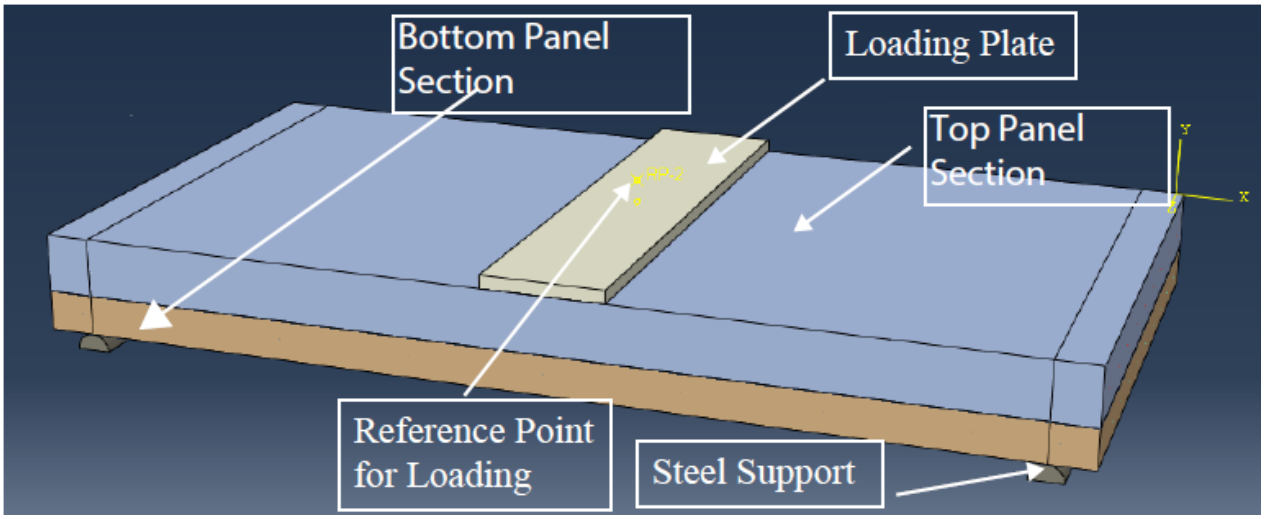

Figure 7.3 FEM model elevation schematic showing supports and loading plate.

The reinforcing bars are modeled as wired truss elements present in ABAQUS. Linear T3D2 material with material properties of the longitudinal reinforcing bars were used to model the reinforcing bar. These longitudinal reinforcing bars have the same total area as the bars in the experimental setup. Longitudinal reinforcing bars are embedded in the concrete surface of the top and bottom sections of the panel to represent the behavior of the reinforcing bars inside the concrete (**Fig.7.4 (a, b)**). Similarly, as done for the reinforcing bars, the 7-wire strand prestressed tendons were modeled as linear T3D2 wired truss elements and were embedded in the bottom slab as shown in **Fig. 7.4(b).** The physical non-linear properties of the tendons are integrated into the numerical model, and an initial predefined stress is applied using predefined stress function in ABAQUS to emulate the initial prestress in the tendons. The material properties of the prestressed tendons used in the finite element model are presented in **Fig. 7.2(b)**. In the FEM model, a vertical displacement of 1.0 in. was applied; a tabular function was used to define the amplitude and loading rate for the monotonic load. The actuator was limited to vertical movement, while movement in all other directions was restricted. The load applied to the reference point of the ABAQUS model was constrained to only allow vertical movement, simulating the actual experimental setup. The explicit analysis solver technique available in ABAQUS was used for the non-linear dynamic analysis.

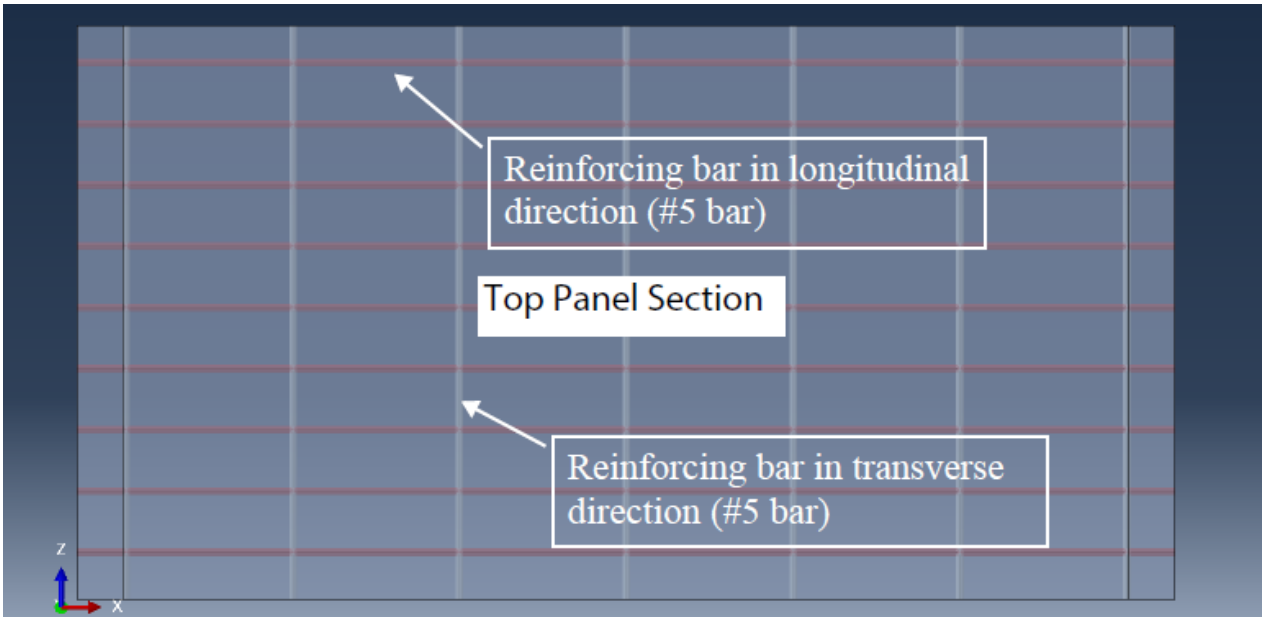

(a)

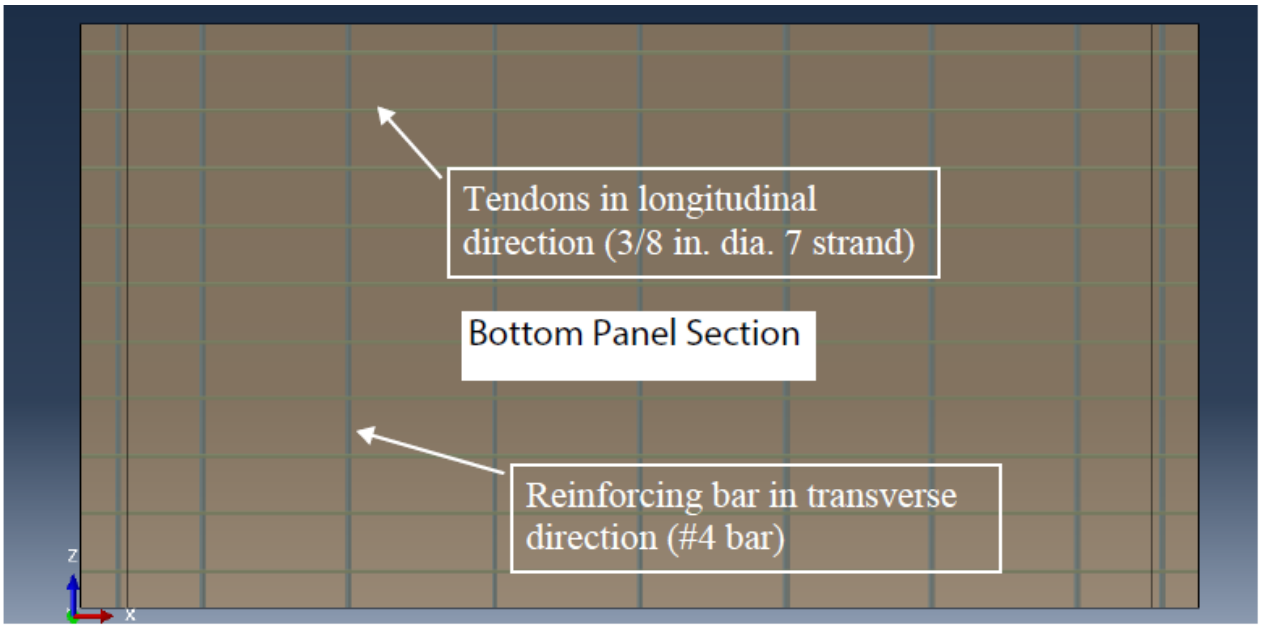

(b)

Figure 7.4 Reinforcing details: (a) top panel section; (b) bottom panel section.

7.3 Numerical Model – Test Panel with No Retrofit

The numerical model was created for the specimen without any retrofit. A vertical load was imposed at the reference point, and both panel sections were meshed with a 1-in. mesh size for all

the solid and wire elements. A mesh sensitivity analysis was conducted for various mesh sizes, and the optimal mesh size, which produced nearly identical results, was selected as the final mesh size for the FEM model. The material properties and model layout detailed in the preceding section were used. As no contact improvement measures were implemented, only frictional contact existed between the two slab surfaces. The interaction between the slab surfaces was simulated using a general friction parameter with a tangential friction coefficient of 0.45 and hard contact in the normal direction. This behavior was replicated in ABAQUS to represent the contact between the two slabs. The 3D view of the meshed structure is shown in **Fig. 7.5.** The elevation of the structure, and the arrangement of the steel reinforcement in the concrete slab is shown in **Fig. 7.6.** **Fig. 7.7** shows the deflected shape of the structure along with the Von-Mises stress.

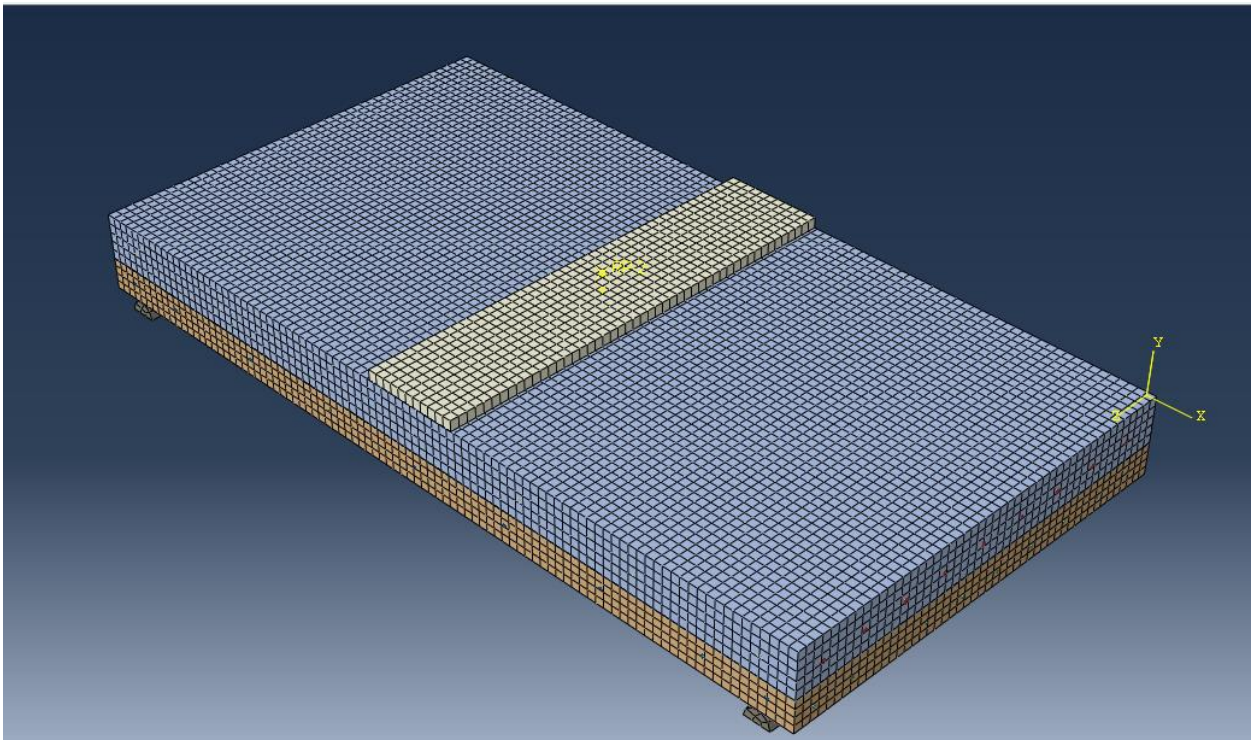

Figure 7.5 Meshed structure of test specimen with no retrofit.

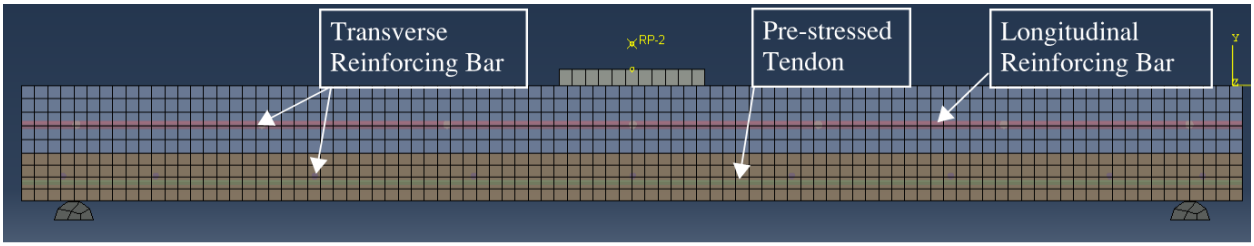

(a)

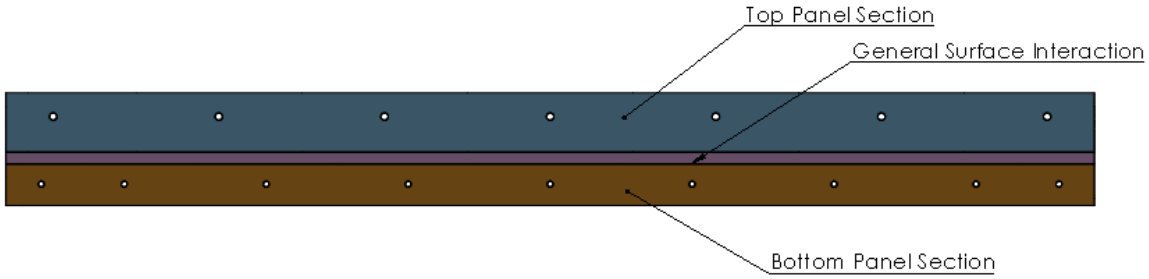

(b)

Figure 7.6 (a) Meshed structure showing elevation and reinforcing bars; and (b) Schematic diagram showing general surface interaction for surface friction.

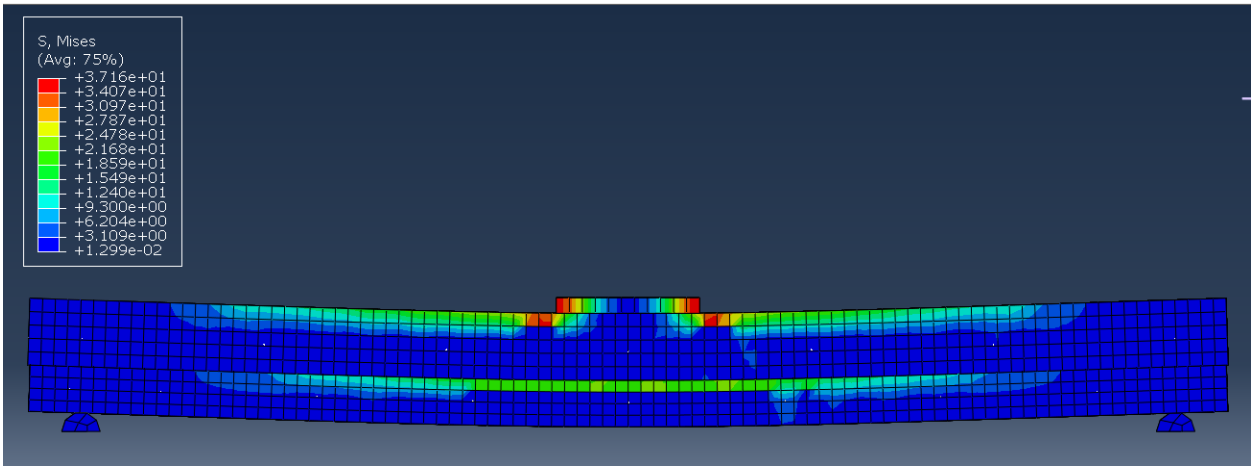

Figure 7.7 Deflected shape with Von- Mises stress (MPa) (1-in. displacement).

The deflected shape closely resembles that of the experimental result. The force-deformation response for the specimen was computed, and a monotonic plot was generated, which was then

compared against the force versus displacement envelope obtained from the experimental study. The results indicate that the FEM model effectively predicts the response of the deck panel, including the delamination effect. It was able to predict the peak load within a 2.0% margin of error and exhibited nearly identical initial stiffness to the experimental study. Minor variations were observed due to geometrical irregularities and construction defects, which were idealized in the FEM model. **Fig. 7.8** shows the comparison of force versus displacement curve from the experiment and the ABAQUS model.

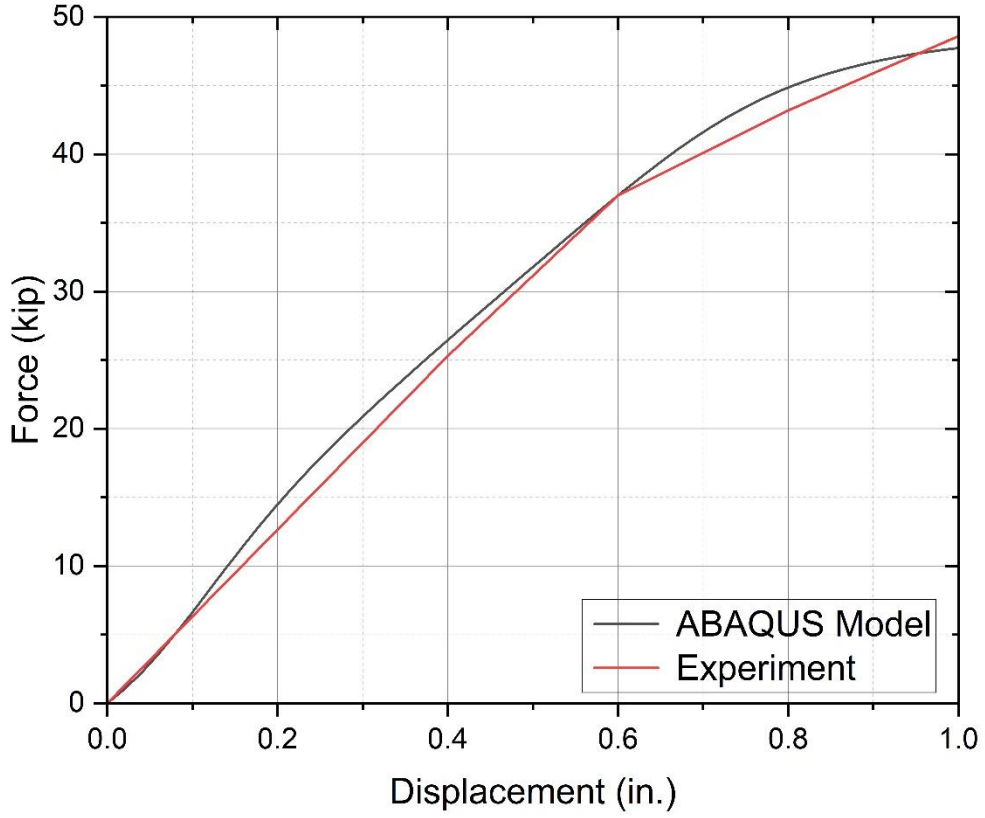

Figure 7.8 Force vs. displacement of test specimen with no retrofit.

7.4 Numerical Model – Epoxy Injection Retrofit Panel

A numerical model was created for the test panels that used the epoxy injection method. The base layout of the numerical model had similar mesh size and loading rate as used in the specimen without any retrofit. To model the behavior of epoxy in ABAQUS, the cohesive modeling technique can be used to define the epoxy adhesive layer. This involves using a surface contact property to define cohesive material properties of the epoxy. The cohesive surface contact represents an adhesive material with a finite thickness. ABAQUS provides the necessary modeling capabilities for this purpose, allowing for the accurate representation of the epoxy behavior within the simulation allowing to input fracture energy of the epoxy and stiffness in the normal, tangential and shear direction. This approach is commonly employed to simulate delamination and adhesion in various material systems (Alfano and Crisfield, 2001). For the FEM model with cohesive element, fracture energy was used that included damage evolution properties of the cohesive element representing epoxy; the stiffness in the normal direction was assumed as 70 ksi and in both tangential directions, the stiffness was assumed as 22 ksi. The 3D model was similar to the model without any retrofit by changing the general surface frictional contact with the properties of cohesive contact. **Fig. 7.9** shows the cohesive surface interaction applied between the two bridge deck panel sections to represent the contact created by the epoxy injection. **Fig. 7.10** shows the deflected shape of the structure along with the Von-Mises stress. **Fig. 7.11** shows the damage initiation in the surface contact element and the damaged epoxy when 1.0-in. vertical displacement is applied on the bridge deck panel.

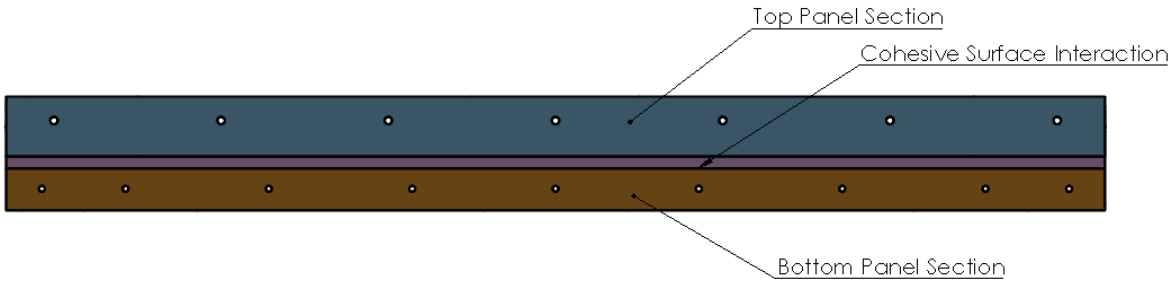

Figure 7.9 Cohesive surface interaction between CIP and PC decks.

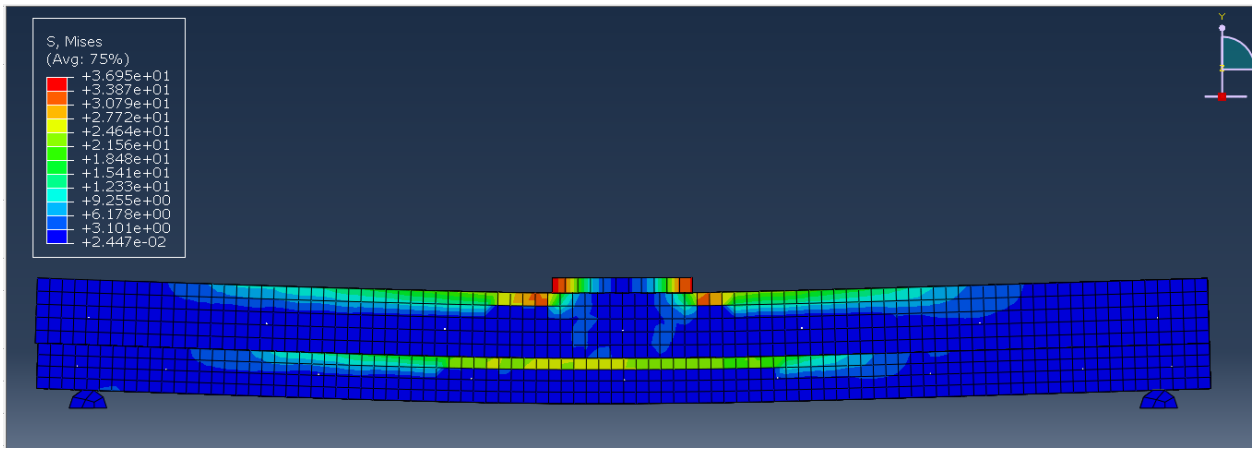

Figure 7.10 Deflected shape of epoxy retrofit specimen with Von- Mises stress (MPa) (1-in. displacement).

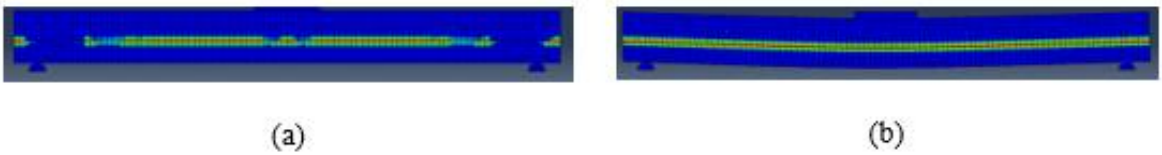

Figure 7.11 Cohesive contact: (a) damage initiation; and (b) damage at vertical deflection of 1.0 in.

The deformed shape closely aligns with that of the experiment. The force-deformation response for the specimen was calculated, and a monotonic load versus displacement plot was generated, which was then compared to the envelope curve from the experimental study. The results indicate that the FEM model effectively predicts the panel response, including damage initiation in the epoxy, lateral load rise due to the inclusion of epoxy, and the delamination effect. The FEM model was able to predict the peak load and initial stiffness, which were almost identical to the experimental study. Minor variations were observed due to geometrical irregularities and constructional defects, which were idealized in the FEM model. **Fig. 7.12** illustrates the comparison of the force-displacement curve from the experiment and the ABAQUS model.

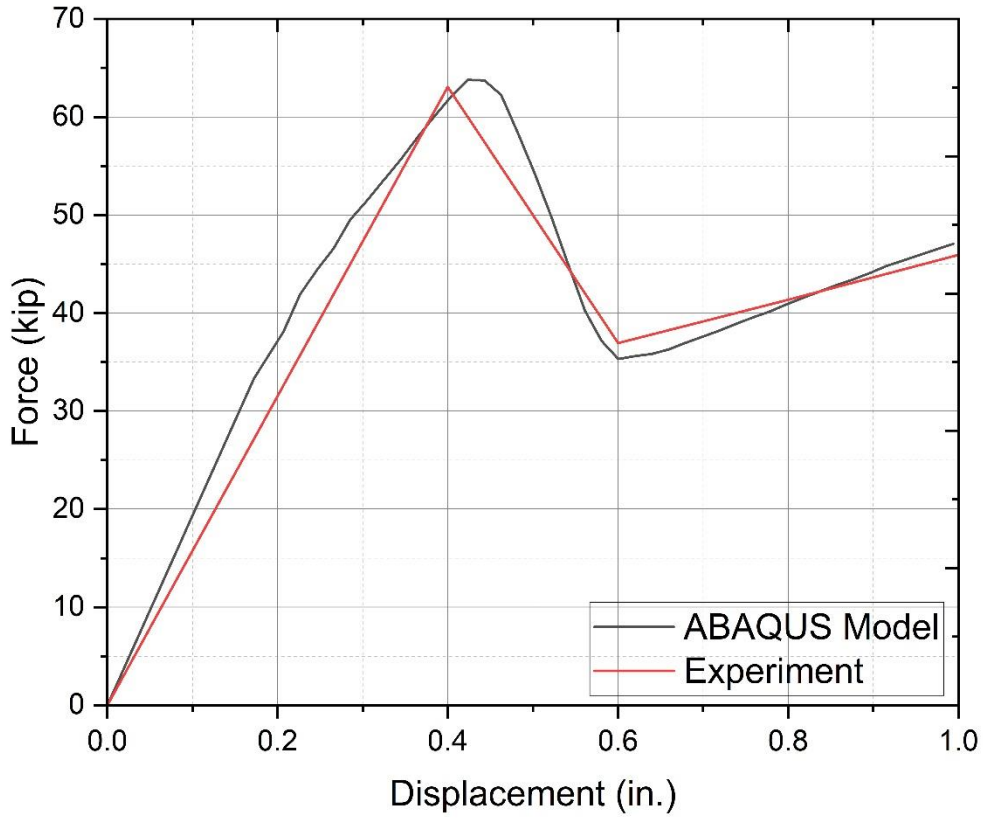

Figure 7.12 Force vs. displacement curve: epoxy injection retrofit.

7.5 Numerical Model – Nonproprietary Shear Anchors

The numerical model was created for the specimen with nonproprietary shear anchors as a retrofit element. Anchors were modeled as elastic elements with a modulus of elasticity equivalent to 29,000 ksi, since no yielding of the anchors was observed during the experiment. Since the anchors were drilled and bonded together with the epoxy, all anchors were embedded in both the CIP and precast sections of the panel. Anchors were modeled as linear wired T3D2 truss elements. The interaction between the panel section surfaces was simulated using a general surface contact friction parameter with a tangential friction coefficient of 0.45 and hard contact in the normal direction. This behavior was replicated in ABAQUS to represent the contact between the two

sections. The 3D view of the meshed structure and bottom panel section showing embedded anchors is shown in **Fig 7.13**. The elevation of the structure and the arrangement of the rebar and prestressed tendons in the concrete panel are shown in **Fig. 7.14.** **Fig. 7.15** shows the deflected shape of the structure along with the Von-Mises stress.

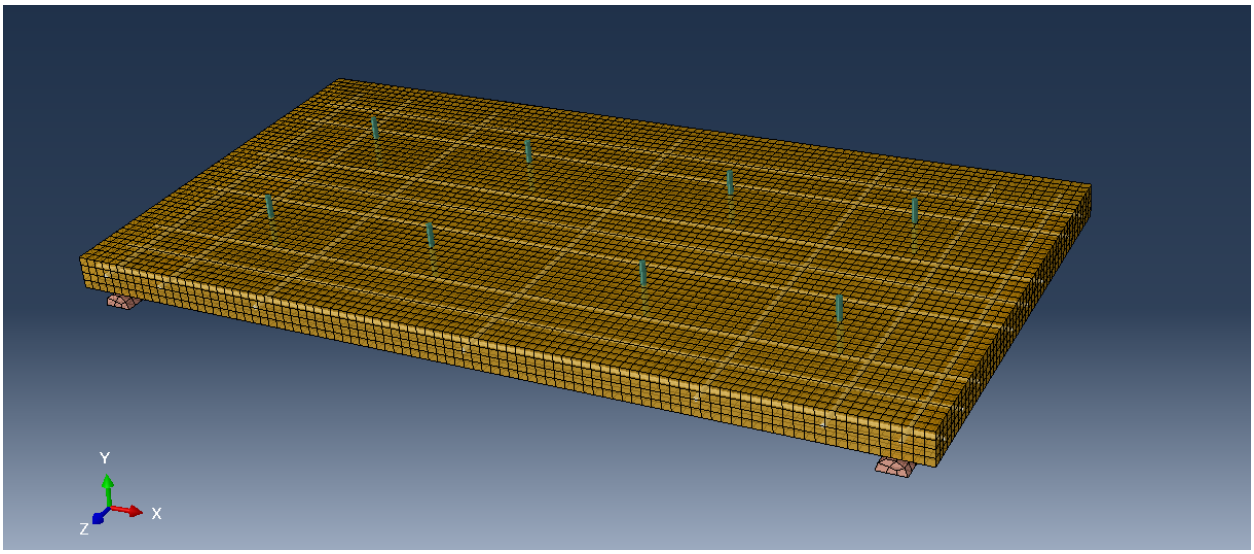

Figure 7.13 Meshed structure of precast panel.

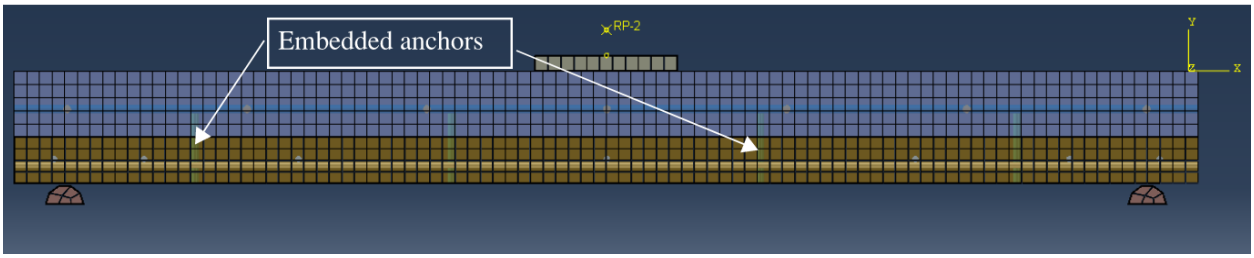

Figure 7.14 Meshed structure showing elevation and embedded anchors.

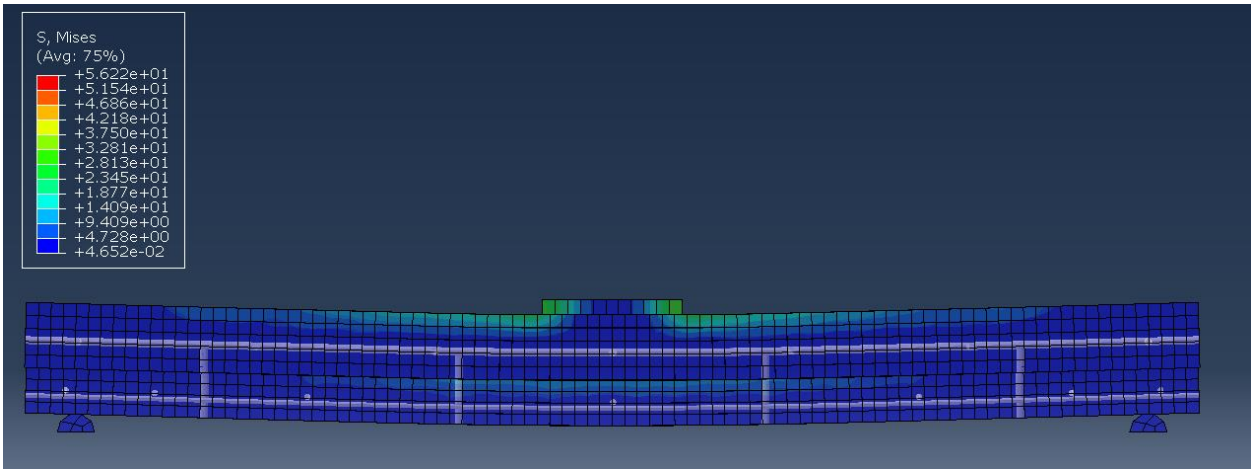

Figure 7.15 Deflected shape with Von- Mises stress (MPa) (1.0-in. displacement).

The deflected shape closely resembles that of the experimental result. The force-deformation response for the specimen was computed, and a monotonic plot was generated, which was compared against the envelope curve obtained from the experiment. The results indicate that the FEM model effectively predicts the response of the deck, including the delamination effect. It could predict the peak and initial stiffness almost identical to the experiment. Minor variations were observed due to geometrical irregularities and constructional defects, which were idealized in the FEM model. **Fig. 7.16** compares the force-displacement curve from the experiment and the curve generated from the ABAQUS model.

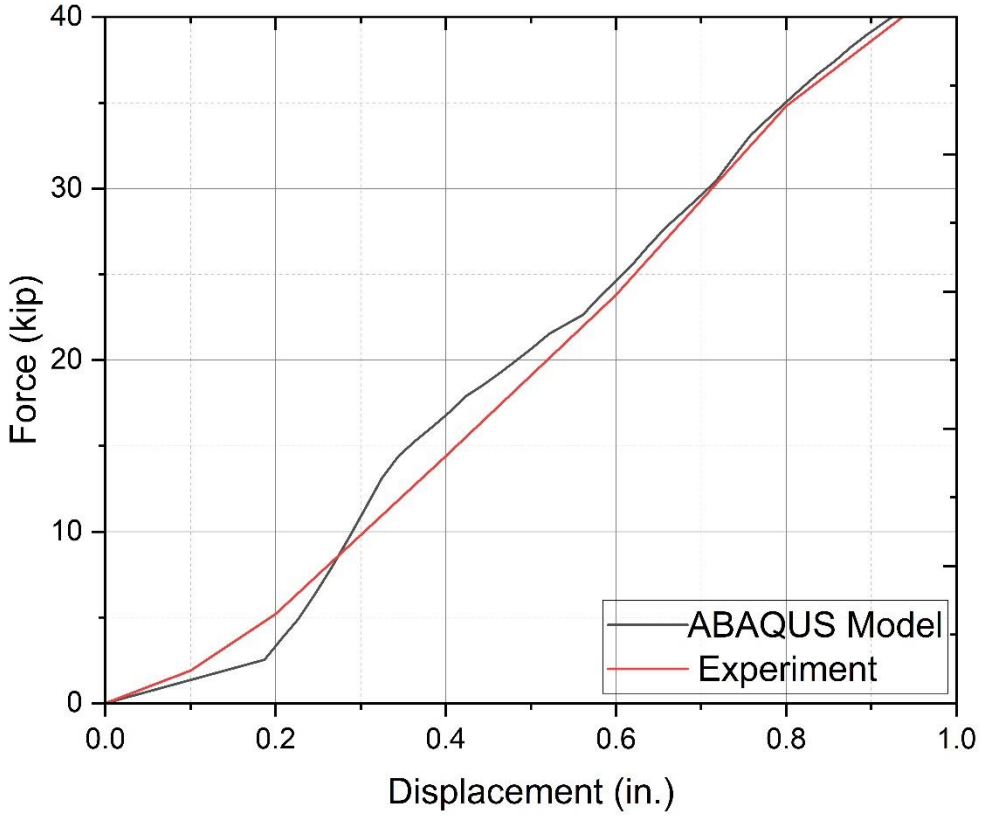

Figure 7.16 Force vs. displacement curve: nonproprietary anchor retrofit.

8 CONCLUSIONS

The study presents a comprehensive analysis regarding the non-composite behavior of concrete bridge decks using partial-depth pre-cast and CIP structural components. This report presents findings from five different methods of retrofitting conventional bridge decks with prestressing cables running parallel to the span between girders. The five retrofit methods would not impact traffic at the surface level. These methods include:

- Uni-directional carbon fiber reinforced polymer composite strips.
- Proprietary shear anchors.
- High modulus epoxy injection.
- Nonproprietary shear anchors.
- Hybrid epoxy injection with proprietary shear anchors.

The testing contained both a quantitative and qualitative analysis to conclude which method would minimize interlayer delamination and separation of the cast-in-place section from the pre-cast section. The performance of each retrofit method was evaluated using the data obtained from the various instruments on each test specimen and compared against the control specimen. The potential impact to the road surface during retrofitting was also evaluated. The test results indicate that all panels using one of the five retrofit methods showed improved performance compared to the test specimen without any retrofit.

8.1 Carbon Fiber Reinforced Polymer

The carbon fiber composite strips were able to improve the flexural capacity and ductile performance of the concrete panel system. Unfortunately, this method of retrofit did not prevent the lateral movement of the CIP section and the improvement was not apparent until the panel had deformed enough for the CFRP strip to resist the load in tension. The CFRP strips were able to resist the large deflection, but they did not significantly minimize the separation of the two panels.

8.2 Proprietary Shear Anchors

The proprietary anchors mechanically bonded the two separate panels, thus creating a composite system. It is important to note that the panel that was fitted with the proprietary anchors had severe separation prior to testing. The low initial stiffness of the panel is a result of this large gap between the two panels. This attribute resulted in a very low overall strength, but the interlayer delamination recorded by the north and south LVDTs were consistent with the desired composite action. The hysteresis curves also indicated that despite a low overall strength the panels were able to recover without a significant loss in strength. Cracking, spalling, and compressive failure were observed before any significant delamination had occurred in specimens retrofitted with these shear anchors.

8.3 Epoxy Injection

During the initial loading cycle of 0.4 in., the concrete test panel showed a significant increase in flexural stiffness, indicating composite action of the deck system, despite the possible presence of a foreign contaminant. Once the epoxy bond had broken, the panel behaved identically to the unmodified panel.

8.4 Nonproprietary Shear Anchors

The nonproprietary shear anchors performed similarly to the proprietary anchorage system as anticipated. The clear advantage of this retrofit is the absence of a third-party vendor. The interlayer delamination of the panels was reduced, the composite action of the panel maintained, and an improvement in overall stiffness was observed.

8.5 Epoxy Injection with Proprietary Shear Anchors

This hybrid method of retrofit involved the use of both epoxy and proprietary shear anchors. The panel's stiffness was significantly improved by the epoxy and any possibility of failure after epoxy bond failure was minimized by the anchors which improved the horizontal shear capacity.

8.6 Recommendations

Even though the hybrid method of epoxy and mechanical anchors showed excellent performance, the bridge decks are not anticipated to see more than 1.0 in. of deflection in service. Bridge decks are not expected to perform within the plastic range and are designed to behave elastically. It is the recommendation of the research team that the epoxy injection method of retrofit should be used to retrofit bridge decks of this type. Not only does this method of retrofit encourage composite action of the panels, but it improves the overall strength. The method also decreases the possibility of water intrusion within the delaminated portion of the panels. Improvements to the salvaged panel and the test specimen highlight the effectiveness of this method.

In addition, the research team would like to make recommendations for future construction of partial-depth bridge decks. All precast panels are to be washed, degreased, and dried before the cast-in-place concrete is poured. Where possible, the precast deck should be free of any snow or ice prior to casting concrete.

REFERENCES

Alfano G., and M.A. Crisfield. (2021). Finite element interface models for the delamination analysis of laminated composites: mechanical and computational issues. *International Journal for Numerical Methods in Engineering* 50, 1701–1736.

Efas, I., Yazdani, N., and Beneberu, E. (2022). Combined load test and NDE: novel method to diagnose and load rate prestressed concrete girder bridges with serviceability issues. *Journal of Bridge Engineering, 27*(10). https://doi.org/10.1061/(ASCE)BE.1943-5592.0001939.

Hieber, D.G., Wacker, J.M., Eberhard, M.O., and Stanton, J.F. (2005). "State-of-the-art report on precast concrete systems for rapid construction of bridges." Washington State Transportation Center (TRAC), Seattle, WA, 112 pg.

Lee, J., and Fenves, G.L. (1998). Plastic damage model for cyclic loading of concrete structures. *Journal of Engineering Mechanics* 124:892-900.

Smith, M. (2019). *ABAQUS/Standard User's Manual, Version 6.9*. Dassault Systèmes Simulia Corp.

Sneed, L., Belarbi, A., and You, Y.M. (2010). "Spalling solution of precast-prestressed bridge deck panels." Missouri Department of Transportation Research, Development and Technology, Jefferson City, MO, 211 pg.

Whittemore, M.D., Stamnas, P.E., and Wellman, R. (2006). "Precast concrete deck panel performance on long span high traffic volume bridges." New Hampshire Department of Transportation, Concord, NH, 42 pg.